

Supporting Information

Metal Ions Trigger the Gelation of Cysteine-Containing Peptide-Appended Coordination Cages

M. Li, H. Zhu, S. Adorinni, W. Xue, A. Heard, A. M. Garcia, S. Kralj, J. R. Nitschke, S. Marchesan**

Supporting Information
©Wiley-VCH 2016
69451 Weinheim, Germany

Metal Ions Trigger the Gelation of Cysteine-Containing Peptide-Appended Coordination Cages

Meng Li,^[a,b,c] Huangtianshi Zhu,^[b] Simone Adorinni,^[c] Weichao Xue,^[b] Andrew Heard,^[b] Ana M. Garcia,^[c] Slavko Kralj,^[d,e] Jonathan R. Nitschke^{[b],*}, and Silvia Marchesan,^{[c,f],*}

WILEY-VCH

SUPPORTING INFORMATION

Table of Contents

Table of Contents	2
1) Materials and methods	3
1.1) General.....	3
1.2) Mass spectrometry (MS).....	3
1.3) Nuclear Magnetic Resonance (NMR)	3
1.4) LC-MS analysis	3
1.5) Circular Dichroism and UV-vis	3
1.6) Oscillatory rheometry.....	4
1.7) Scanning Electron Microscopy (SEM)	4
1.8) Raman Spectroscopy	5
1.9) Transmission Electron Microscopy (TEM)	5
2) Synthesis	5
2.1) Peptide B , <i>p</i> -aminobenzoyl-L-Phe-D-Cys-L-Phe-NH ₂	5
2.2) Peptide C , <i>p</i> -aminobenzoyl-L-Phe-D-Phe-L-Cys-NH ₂	8
2.3) Peptide D , <i>p</i> -aminobenzoyl-L-Phe-D-Met-L-Phe-NH ₂	12
2.4) Peptide C analog, <i>N</i> -Ac-L-Phe-D-Phe-L-Cys-NH ₂	14
2.5) Enantiomer of peptide C , <i>p</i> -aminobenzoyl-D-Phe-L-Phe-D-Cys-NH ₂	17
2.6) Cage 1	19
2.7) Cage 2	23
2.8) Cage 3	27
2.9) Circular Dichroism	33
3) Gels formation and characterization	37
3.1) General preparation of cage gel	37
3.2) General preparation of cage gels triggered by metal ions	37
3.3) Oscillatory rheometry of Cage 2 gel triggered by metal ions	38
3.4) TEM characterization.....	39
3.5) Raman spectroscopy	40
3.6) XPS analysis	40
References:	41
CRedit:.....	41

1) Materials and methods

1.1) General

2-chlorotrityl chloride resin, *O*-benzotriazole-*N,N,N,N*-tetramethyluronium-hexafluoro-phosphate (HBTU), 1-hydroxy-7-azabenzotriazole (HOAt) and the Fmoc-protected amino acids were purchased from GL Biochem (Shanghai) Ltd. (Shanghai, China). All other reagents and solvents were purchased from commercial suppliers and were used as supplied without purification unless stated otherwise. Iron(II)bis(trifluoromethane)sulfonimide, peptide *p*-aminobenzoyl-L-Phe-D-Cys-L-Phe-NH₂ **B** and Peptide *p*-aminobenzoyl-L-Phe-D-Phe-L-Cys-NH₂ **C** were prepared following literature procedures.^[S1] Peptide *p*-aminobenzoyl-L-Phe-D-Met-L-Phe-NH₂ **D** was purchased from Sangon Biotech (Shanghai) Co., Ltd. Cage **1**, **2**, **3** were synthesized following literature procedures.^[S2]

1.2) Mass spectrometry (MS)

High resolution electrospray mass spectra (HR ESI-MS) were obtained on a Waters Synapt G2-Si instrument.

1.3) Nuclear Magnetic Resonance (NMR)

NMR spectra were recorded on a Bruker 400 MHz Avance III HD Smart Probe, Bruker 500 MHz AVIII HD Smart Probe Spectrometer and Bruker 500 MHz DCH Cryoprobe Spectrometer. Proton chemical shift (δ) values are reported in ppm relative to the solvent residual acetonitrile peak ($\delta = 1.94$ ppm). Carbon chemical shift (δ) values are reported in ppm relative to the solvent residual peak ($\delta = 1.32$ and 118.26 ppm for CH₃CN). Coupling constants (*J*) are reported in Hertz (Hz) and the signal multiplicities are described as: s (singlet), d (doublet), t (triplet), m (multiplet) and b (broad).

The solvodynamic radius (*R*) from DOSY analysis has been calculated using the Stokes-Einstein equation (1):

$$D = \frac{k_B T}{6\pi\eta R} \quad (1)$$

Where *D* is the diffusion coefficient calculated from DOSY, *k_B* is the Boltzmann constant, *T* is the absolute temperature, and η is the viscosity of the solvent.

1.4) LC-MS analysis

LC-MS data was acquired on an Agilent 6120 LC-MS system with a C-18 analytical column (Zorbax SB-C18 Rapid Resolution HT 2.1x50 mm, particle size: 1.8 microns), flow 0.5 ml/min. The gradient used consisted of CH₃CN/H₂O with 0.1% formic acid with the following program: *t* = 0-2 min. 5% CH₃CN; *t* = 10 min. 95% CH₃CN; *t* = 12 min. 95% CH₃CN (peptide *t_R* = 8.4 min).

1.5) Circular Dichroism and UV-vis

UV-vis measurements were employed to fine-tune the solution concentration for subsequent CD measurements, and were performed on a Varian Cary 400 scan UV-vis spectrophotometer with a 1 mm path-length cuvette at 25 °C. Circular Dichroism was performed on an Applied-Photophysics Chirascan CD spectrometer using a 1 mm path-length cuvette. Experiments were recorded at 298 K, maintained with a Peltier temperature control. Measurements were background subtracted from blank solvent in an identical cuvette. The sample concentrations were adjusted to maintain a HV below 800 V.

SUPPORTING INFORMATION

1.6) Oscillatory rheometry

Dynamic time sweep rheological analyses were performed on a Malvern Kinexus Ultra Plus Rheometer (Alfatest, Milan, Italy) with a 20 mm stainless steel parallel plate geometry. The system was kept at 25 °C using a Peltier temperature controller. Each gel was prepared in situ and immediately analyzed with a gap of 0.8 mm. Time sweeps were recorded for 1 hour, using a frequency of 2 Hz and a controlled stress of 2 Pa. After 1 hour, frequency sweeps were recorded from 0.1 to 20 Hz using a controlled stress of 2 Pa. Finally, stress sweeps were recorded using a frequency of 2 Hz until the breaking point for every gel, recognizable by the inversion of G' and G'' values.

Shear modulus

The three gels were analysed using the generalized Maxwell model, which assumes that the pure elastic behaviour could be represented by a spring and the pure liquid behaviour by a dashpot, according to eqs. (2) and (3),

$$G' = G_e + \sum_{i=1}^n G_i \frac{(\lambda_i \omega)^2}{1 + (\lambda_i \omega)^2}; G_i = \frac{n_i}{\lambda_i} \quad (2)$$

$$G'' = \sum_{i=1}^n G_i \frac{(\lambda_i \omega)}{1 + (\lambda_i \omega)^2}; G_i = \frac{n_i}{\lambda_i} \quad (3)$$

In the equations, we consider n Maxwell elements. Here are expressed the dependencies of G' and G'' for the spring constant (G_i), dashpot viscosity, and relaxation time. The selection of the number of Maxwell elements is based on a statistical procedure that tend to minimize the difference between the empirical and theoretical behaviour, represented by an error X^2/Np , the product between the sum of square errors and the number of fitting parameters. The fundamental assumption of the fitting is that relaxation times are not independent of each other, all scaled by a factor 10. ($\lambda_{i+1} = \lambda_i * 10$)

From G' and G'' we can calculate the shear modulus G by equation (4).

$$G = G_e + \sum_{i=1}^n G_i \quad (4)$$

 γ critical

For strain sweep fitting curves, we consider the Soskey-Winter equation (5), a model where:

$$G' = G'_0 \frac{1}{1 + (b\gamma)^n} \quad (5)$$

When γ tend to zero we evaluate the term G'_0 , b and n are adjustable parameters to fit empirical and theoretical model. Gamma critical represent the passage to strain softening behaviour, making a limit to the linear regime and arbitrarily determined as $\gamma_c = G'/G'_0 = 0.95$.

1.7) Scanning Electron Microscopy (SEM)

SEM analyses were performed on a Gemini 300, ZEISS (Germany) equipped with an Oxford Instruments INCS X-Act energy-dispersive X-ray spectroscopy (EDXS) detector. SEM grids (copper-grid-supported lacey carbon film) were first exposed to the UV-ozone cleaner (UV-Ozone Procleaner Plus) for 10 mins to make the grid surface more hydrophilic. Seven-day aged gels were precisely deposited on a SEM grid and dried for 15 mins at room temperature.

SUPPORTING INFORMATION

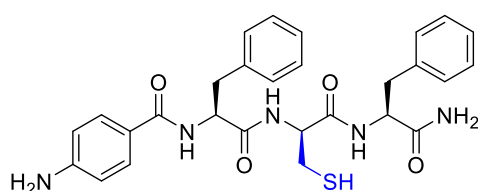
1.8) Raman Spectroscopy

Raman analysis was undertaken with an Invia Renishaw microspectrometer (50) equipped with He-Ne laser at 532 nm. The laser was focused using a 50x microscope and the power of the laser was set as required for the sample. At least 10 spectra per sample were acquired to insure the homogeneity of the samples. For the characterization of the gels, a small piece of gel was deposited on a glass microscope slide and open-air dried before the analysis.

1.9) Transmission Electron Microscopy (TEM)

Samples were prepared by settling the gels on copper-lacey carbon film grids, using uranyl acetate as a negative stain. The grids were previously treated by exposing them to UV-Ozone cleaner (*UV-Ozone Procleaner Plus*) for 5 minutes to increase surface hydrophilicity. TEM images were acquired using a Jeol JEM 2100 (Japan) instrument at 100 kV. The average diameter of the nanostructures was derived by considering at least 100 objects from various micrographs using FIJI2 software.

2) Synthesis

2.1) Peptide B, *p*-aminobenzoyl-L-Phe-D-Cys-L-Phe-NH₂

p-Aminobenzoyl-L-Phe-D-Cys-L-Phe-NH₂ was synthesized following Fmoc-based solid-phase peptide synthesis (SPPS) under a dry and inert atmosphere. The swelling of the resin (2-chlorotrytil chloride, 0.5 g) was done in dichloromethane (5 mL). Then SOCl₂ (50 μ L) was added, and the reaction was shaken under an argon flow for 1 h. After that, the resin was washed with DMF (3 \times 5 mL) and dichloromethane (3 \times 5 mL). Next, a solution of Fmoc-Rink amide linker (0.43 g, 0.8 mmol), *N,N*-diisopropylethylamine (DIPEA) (0.45 mL) in DMF/dichloromethane (3:2) was added to the resin, and the reaction was stirred for 3 h. Then, methanol (1 mL) was added and it was shaken for 10 minutes following by washes with DMF (3 \times 5 mL) and dichloromethane (3 \times 5 mL). For the deprotection, 20% piperidine in DMF (5 mL) was added to the reactor and stirred at room temperature (2 \times 10 minutes). The reaction mixture was washed with DMF and dichloromethane. For the first coupling, a mixture of Fmoc-L-Phe-OH (0.7 g, 1.8 mmol), HBTU (0.46 g, 1.2 mmol), HOAt (0.16 g, 1.2 mmol) and DIPEA 1 M in DMF (1 mL) in DMF was ultrasonicated until the solution was clear, and was added to the reactor. The coupling was shaken at room temperature for 1.5 h. Then, the resin was washed and deprotected as in the previous step. The coupling and deprotection of the following amino acids (D-Cys and L-Phe) were performed using 2,4,6-trimethylpyridine 0.5 M in DMF (1 mL), by using Fmoc-D-Cys-OH (1.05 g, 1.8 mmol) for the second coupling and Fmoc-L-Phe-OH (0.7 g, 1.8 mmol) for the third one. For the introduction of *p*-aminobenzoyl motif, coupling was performed under the same conditions by using Boc-protected *p*-aminobenzoic acid instead of an Fmoc-protected amino acid. The peptide was cleaved from the resin by shaking 2 h in the presence of a solution of trifluoroacetic acid (TFA)/DCM/H₂O/triisopropylsilane (47.5/47.5/2/3) (10 mL). The solution was drained from the reactor, and the solvent was evaporated under Ar flow. The remaining oil was dissolved in a mixture of acetonitrile/H₂O containing 0.05% TFA, and then purified by reverse-phase HPLC (Agilent Technologies, Santa Clara, CA, USA). The HPLC Agilent 1260 Infinity system was equipped with a preparative gradient pump (1311B), semipreparative C-18 column (Kinetex, 5 microns, 100 \AA , 250 mm \times 10 mm, Phenomenex, Torrance, CA, USA), autosampler (G1329B), and Photodiode Array detector (G1315C). The following HPLC method was used for the purification of the peptide: $t = 0$ -2 min, 35% CH₃CN; $t = 14$ min, 65% CH₃CN; $t = 16$ min, 95% CH₃CN; $t = 17$ min, 95% CH₃CN. The compound was then freeze-dried to yield the corresponding peptide as a white fluffy powder. Peptide identity was verified by ESI-MS, ¹H-NMR, and ¹³C-NMR.

¹H NMR (500 MHz, DMSO-*d*₆, 298 K) δ 8.34 – 8.18 (m, 3H, CONH), 7.56 (d, $J = 8.2$ Hz, 2H, ArH), 7.39 (s, 1H, CONH₂), 7.31 (d, $J = 7.3$ Hz, 2H, ArH), 7.24 (dd, $J = 7.6$ Hz, 2H, ArH), 7.23 – 7.07 (m, 7H, ArH), 6.55 (d, $J = 8.5$ Hz, 2H, ArH), 4.61 – 4.55 (m, 1H, α CH),

SUPPORTING INFORMATION

4.42 – 4.37 (m, 1H, α CH), 4.30 (ddd, $J = 7.9, 4.7$ Hz, 1H, α CH), 3.10 – 2.99 (m, 3H, β CH), 2.77 (dd, $J = 13.7, 10.5$ Hz, 1H, β CH), 2.56 (dd, $J = 4.4$ Hz, 1H, β CH), 2.47 – 2.41 (m, 1H, β CH), 1.54 (dd, $J = 9.2, 7.9$ Hz, 1H, SH).

^{13}C NMR (126 MHz, $\text{DMSO-}d_6$, 298 K) δ 172.9, 172.0, 169.2, 166.8 (4 x CO); 138.3, 138.1, 129.3, 129.2, 129.2, 128.2, 128.1, 126.3, 126.3, 113.3, (Ar); 55.6, 54.7, 54.3, (α C); 37.6, 37.1, 26.2 (β C).

ESI-MS: m/z $[\text{M} + \text{H}]^+$ 534.2161, $[\text{M} + \text{Na}]^+$ 556.1990.

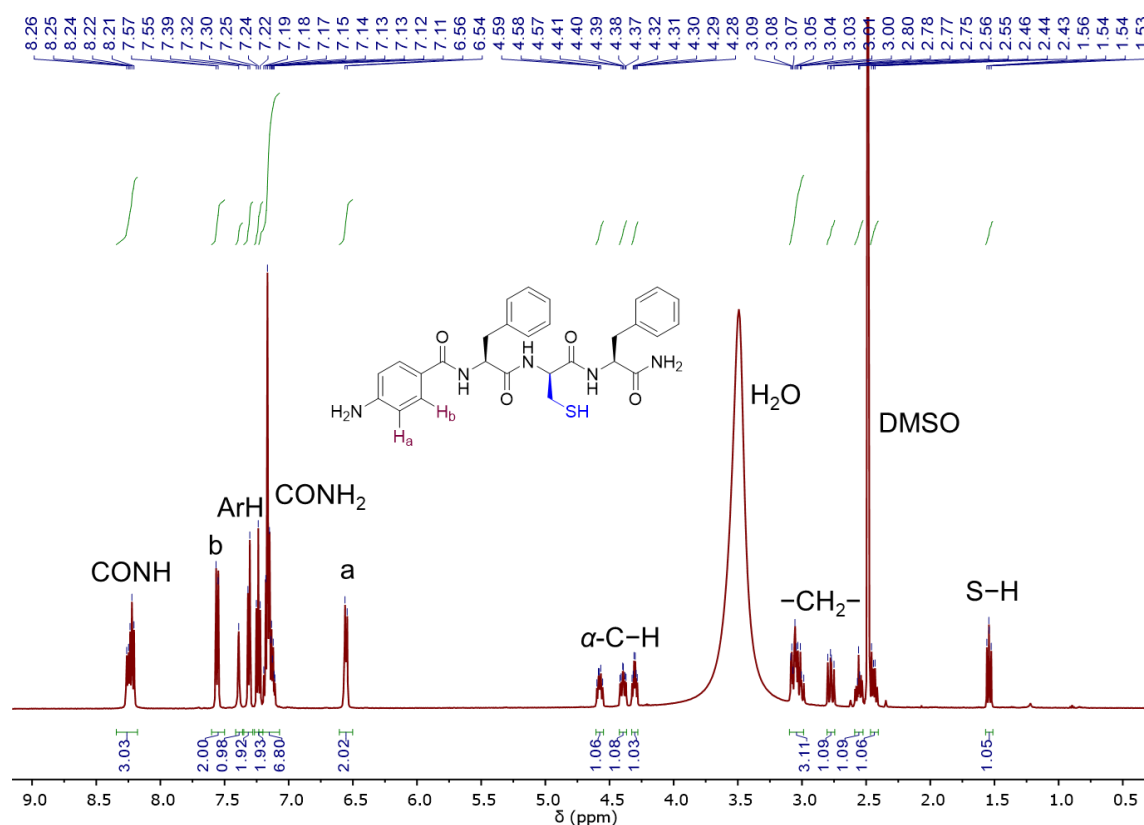


Figure S1: ^1H NMR spectrum (500 MHz, 298 K, $\text{DMSO-}d_6$) of the peptide B.

SUPPORTING INFORMATION

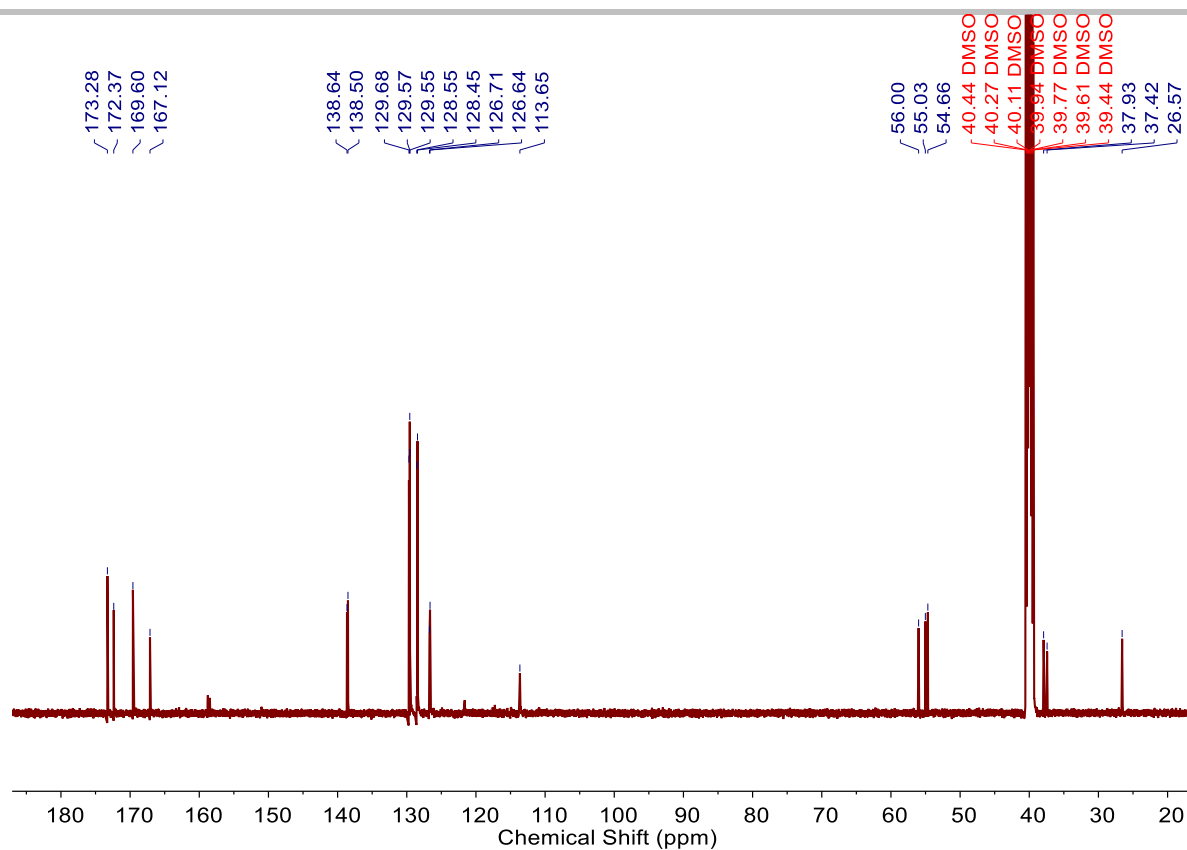


Figure S2: ¹³C NMR spectrum (126 MHz, 298 K, DMSO-*d*₆) of the peptide B.

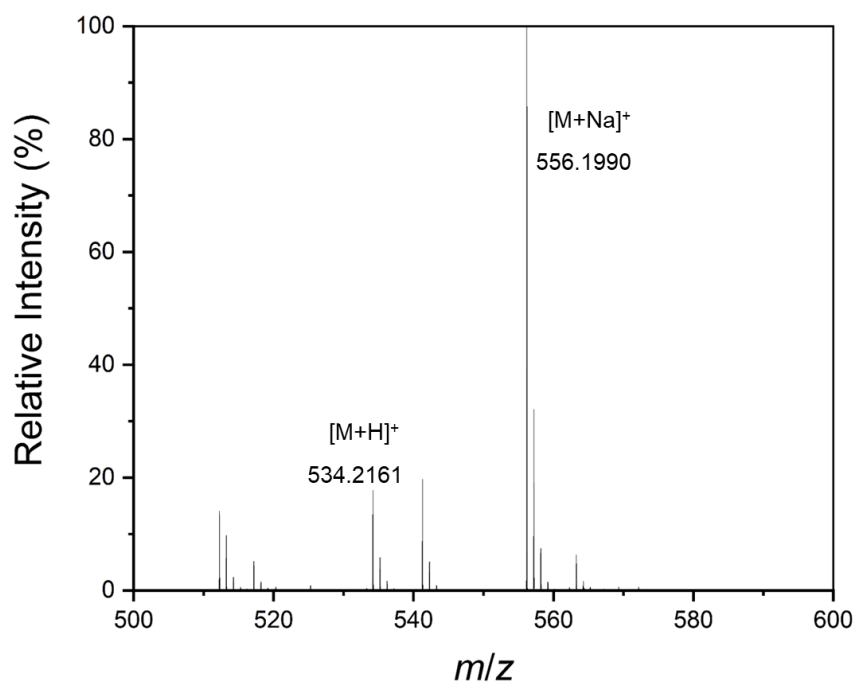
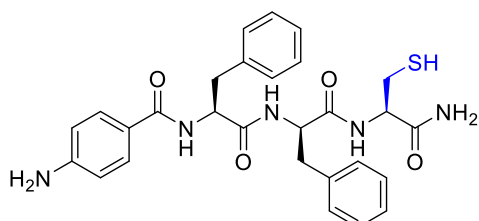


Figure S3: ESI-MS spectrum of the peptide B.

SUPPORTING INFORMATION

2.2) Peptide C, *p*-aminobenzoyl-L-Phe-D-Phe-L-Cys-NH₂

p-Aminobenzoyl-L-Phe-D-Cys-L-Phe-NH₂ was synthesized following Fmoc-based SPPS under dry and inert atmosphere. The swelling of the resin (2-chlorotrytil chloride, 0.5 g) was done in dichloromethane (5 mL). Then SOCl₂ (0.5 μL) was added, and the reaction was shaken under an argon flow for 1 h. After that, the resin was washed with DMF (3 × 5 mL) and dichloromethane (3 × 5 mL). Next, a solution of Fmoc-Rink amide linker (0.43 g, 0.8 mmol), 2,4,6-trimethylpyridine (0.90 mL) in

DMF/dichloromethane (1:1) was added to the resin, and the reaction was stirred for 1.5 h. Then methanol (1 mL) was added and it was shaken for 5 minutes followed by washes with DMF (3 × 5 mL) and dichloromethane (3 × 5 mL). For the deprotection, piperidine 20% in DMF (5 mL) was added to the reactor and was stirred at room temperature (2 × 10 minutes). The reaction mixture was washed with DMF and dichloromethane. For the first coupling, a mixture of Fmoc-L-Cys-OH (1.05 g, 1.8 mmol), HBTU (0.46 g, 1.2 mmol), HOAt (0.16 g, 1.2 mmol) and 2,4,6-trimethylpyridine 0.5 M in DMF (1.2 mL) was ultrasonicated until the solution was clear, and was added to the reactor. The coupling was shaken at room temperature for 1.5 h. Then, the resin was washed and deprotected as in the previous step. The coupling and deprotection of the following amino acids (D-Phe and L-Phe) were done exactly the same way as the first coupling, by using Fmoc-D-Phe-OH (0.7 g, 1.8 mmol) for the second coupling and Fmoc-L-Phe-OH (0.7 g, 1.8 mmol) for the third one. For the introduction of *p*-aminobenzoyl motif, a coupling was performed under the same conditions by using Boc-protected *p*-aminobenzoic acid instead of a Fmoc-protected amino acid. Eventually, the peptide was cleaved from the resin by shaking 2 h in the presence of a solution of TFA/DCM/H₂O/triisopropylsilane (47.5/47.5/2/3) (10 mL). The solution was drained from the reactor, and the solvent was evaporated under air flow. The remaining oil was dissolved in a mixture of acetonitrile/H₂O (containing 0.05% of TFA), and then purified by reverse-phase HPLC (Agilent Technologies, Santa Clara, CA, USA). The HPLC Agilent 1260 Infinity system was equipped with a preparative gradient pump (1311B), semipreparative C-18 column (Kinetex, 5 microns, 100 Å, 250 mm × 10 mm, Phenomenex, Torrance, CA, USA), autosampler (G1329B), and Photodiode Array detector (G1315C). The following HPLC method was used for the purification of the peptide: t = 0–2 min, 35% CH₃CN; t = 14 min, 65% CH₃CN; t = 16 min, 95% CH₃CN; t = 17 min, 95% CH₃CN. The compound was then freeze-dried to yield the corresponding peptide as a white fluffy powder. Peptide identity was verified by ESI-MS, ¹H-NMR, and ¹³C-NMR.

¹H NMR (500 MHz, DMSO-*d*₆, 298 K) δ 8.41 (d, *J* = 8.2 Hz, 1H, CONH), 8.21 (d, *J* = 8.4 Hz, 1H, CONH), 8.03 (d, *J* = 7.4 Hz, 1H, CONH), 7.50 (d, *J* = 8.6 Hz, 2H, ArH), 7.38 (s, 1H, CONH₂), 7.25 (d, *J* = 7.1 Hz, 2H, ArH), 7.22 – 7.17 (m, 6H, ArH), 7.16 – 7.09 (m, 2H, ArH), 6.54 (d, *J* = 8.5 Hz, 2H, ArH), 4.60 – 4.50 (m, 2H, αCH), 4.34 – 4.28 (m, 1H, αCH), 3.06 (dd, *J* = 13.6, 4.7 Hz, 1H, βCH), 2.83 – 2.65 (m, 5H, βCH), 2.07 (dd, *J* = 9.2, 7.9 Hz, 1H, SH).

¹³C NMR (126 MHz, DMSO-*d*₆, 298 K) δ 172.0, 171.5, 171.1, 166.5, (4 × CO); 138.5, 137.8, 129.4, 129.2, 129.1, 128.1, 126.4, 126.2, 113.12, (Ar); 55.2, 55.00, 54.1, (3 × αC); 37.8, 37.0, 26.2 (3 × βC).

ESI-MS: *m/z* calculated for M = 533.2097, observed positive mode [M + H]⁺ = 534.2171 and [M + Na]⁺ = 556.2000.

SUPPORTING INFORMATION

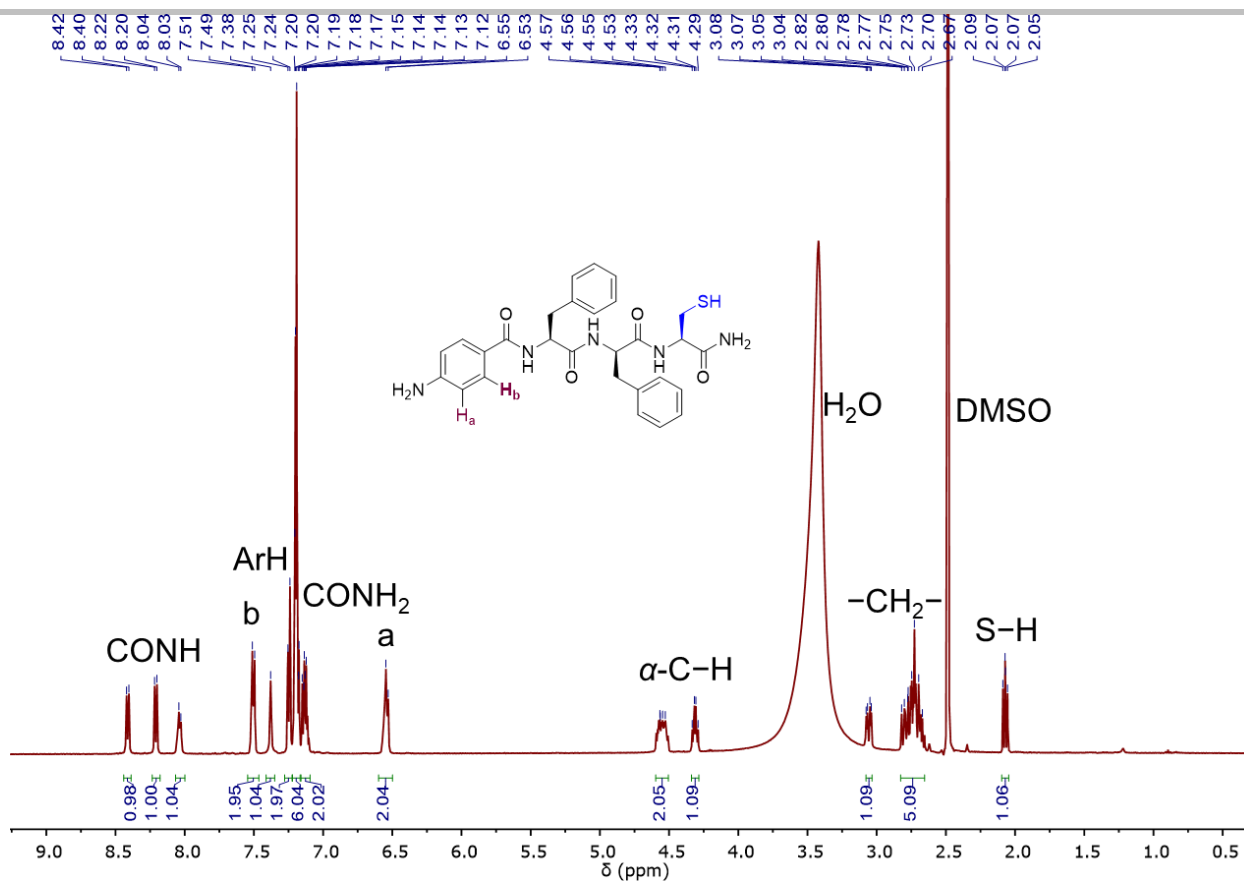


Figure S4: ^1H NMR spectrum (500 MHz, 298 K, $\text{DMSO-}d_6$) of the peptide C.

SUPPORTING INFORMATION

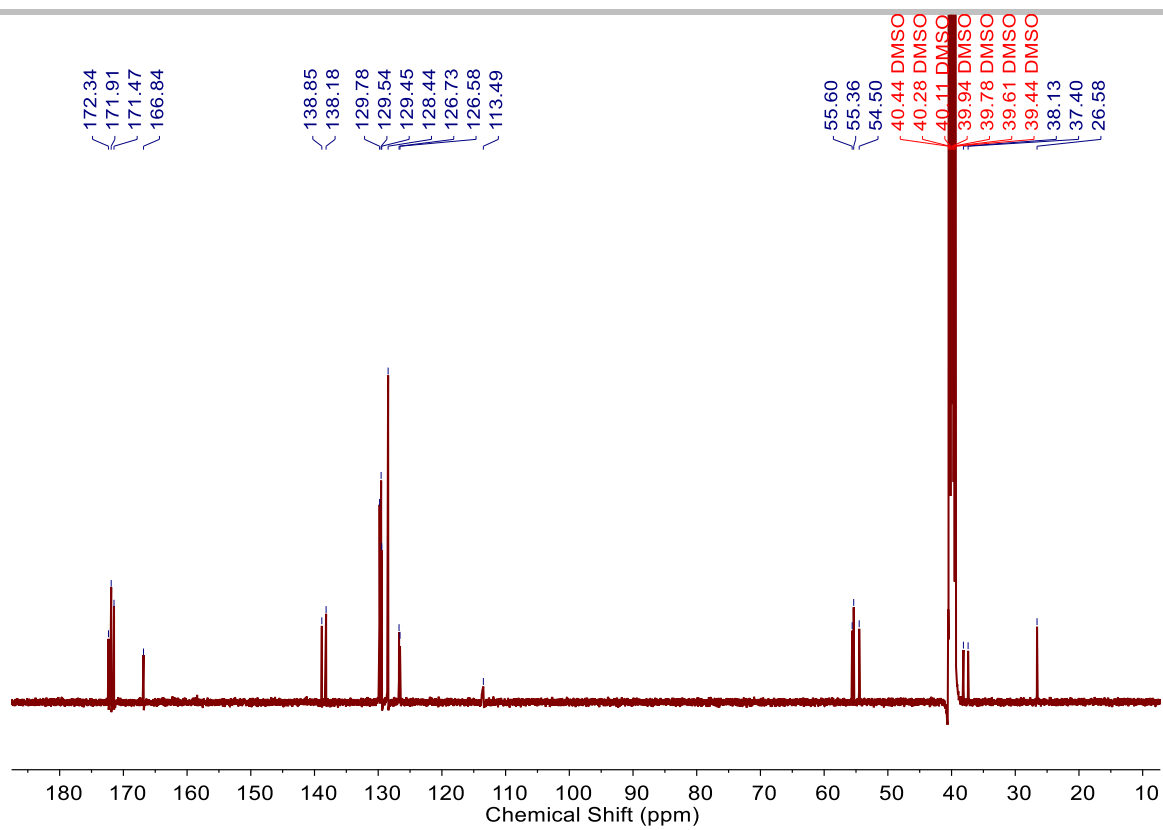


Figure S5: ^{13}C NMR spectrum (126 MHz, 298 K, $\text{DMSO-}d_6$) of the peptide C.

SUPPORTING INFORMATION

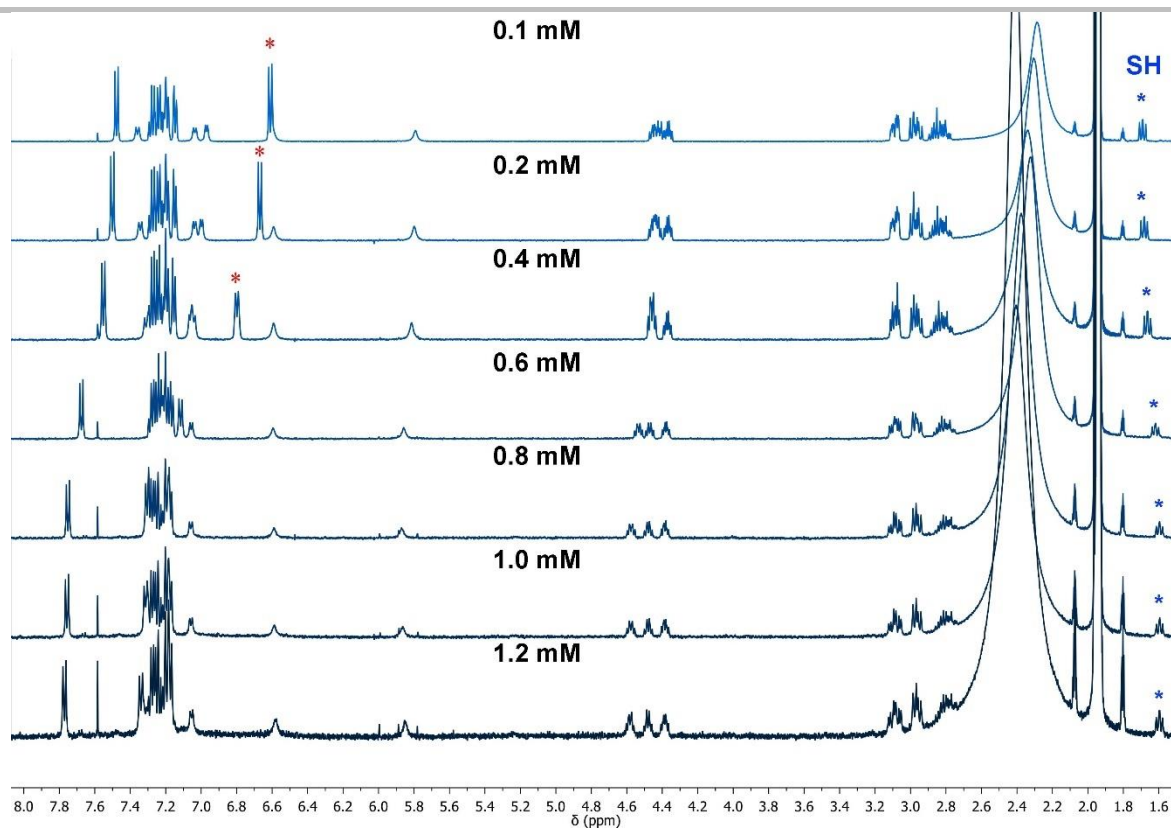


Figure S6: ^1H NMR spectra (500 MHz, 298 K, $\text{DMSO-}d_6$) of the peptide **C** (1.2 mM) and different concentrations of Ag^+ (0.1, 0.2, 0.4, 0.6, 0.8, 1.0, 1.2 mM).

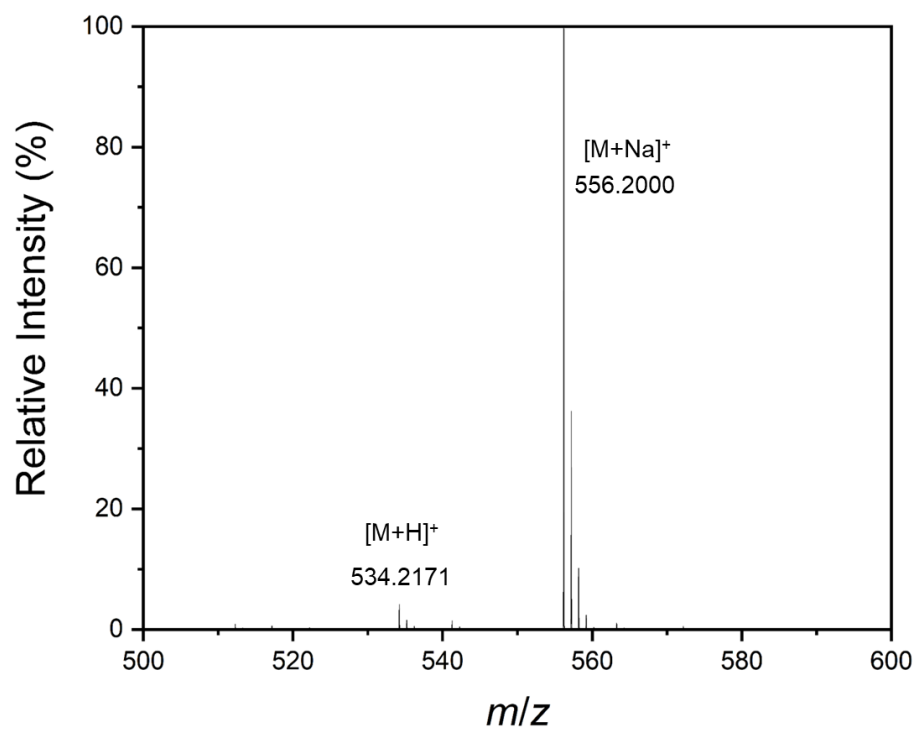
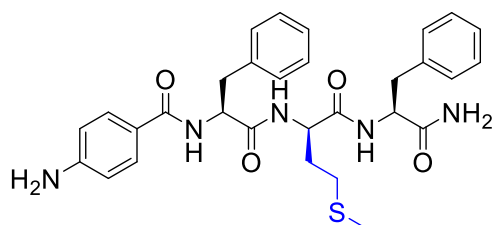


Figure S7: ESI-MS spectrum of the peptide **C**.

SUPPORTING INFORMATION

2.3) Peptide D, *p*-aminobenzoyl-L-Phe-D-Met-L-Phe-NH₂

p-Aminobenzoyl-L-Phe-D-Met-L-Phe-NH₂ was purchased from Shanghai Biotech Company and fully characterised by ¹H-NMR, ¹³C-NMR and ESI-MS.

¹H NMR (500 MHz, DMSO-*d*₆, 298 K) δ 8.24 (d, J = 7.1 Hz, 1H, CONH), 8.19 (dd, J = 8.5, 2.6 Hz, 2H, CONH), 7.57 (d, J = 8.7 Hz, 2H, ArH), 7.36 (s, 1H, CONH₂), 7.30 – 7.26 (m, 2H, ArH), 7.23 (dd, J = 7.6 Hz, 2H, ArH), 7.20 – 7.09 (m, 7H, ArH), 6.56 (d, J = 8.7 Hz, 2H, ArH), 4.53 (dd, J = 7.5 Hz, 1H, α CH), 4.39 – 4.34 (m, 1H, α CH), 4.18 (ddd, J = 8.6, 4.3 Hz, 1H, α CH), 3.09 – 3.05 (m, 1H, β CH), 3.00 (d, J = 8.5 Hz, 2H, β CH), 2.78 – 2.72 (m, 1H, β CH), 1.91 (dd, J = 8.6, 6.9 Hz, 2H, δ CH₂), 1.88 (s, 3H, SCH₃), 1.71 – 1.65 (m, 1H, γ CH), 1.46 (ddd, J = 14.2, 6.7, 1.7 Hz, 1H, γ CH).

¹³C NMR (126 MHz, DMSO-*d*₆, 298 K) δ 173.1, 171.9, 170.7, 166.7, (4 x CO); 138.3, 138.0, 129.3, 129.2, 129.1, 128.2, 128.0, 126.4, 126.2, 121.4, 113.4, (Ar); 55.7, 54.3, 51.7, (3 x α C); 37.4, 37.2, 31.3, (3 x β C); 29.1 (γ C); 14.5 (δ C).

ESI-MS: m/z calculated for M = 561.2410, observed positive mode [M + Na]⁺ = 584.2266.

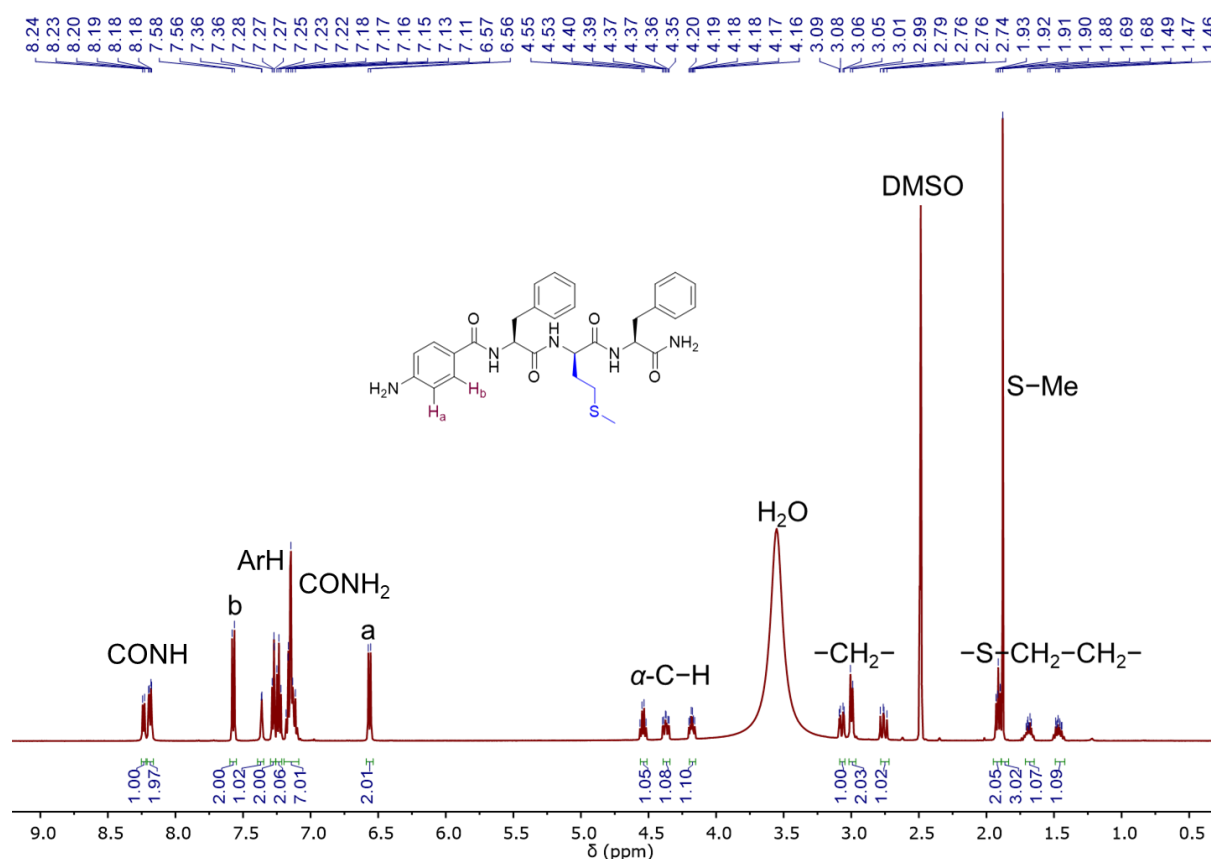


Figure S8: ¹H NMR spectrum (500 MHz, 298 K, DMSO-*d*₆) of the peptide D.

SUPPORTING INFORMATION

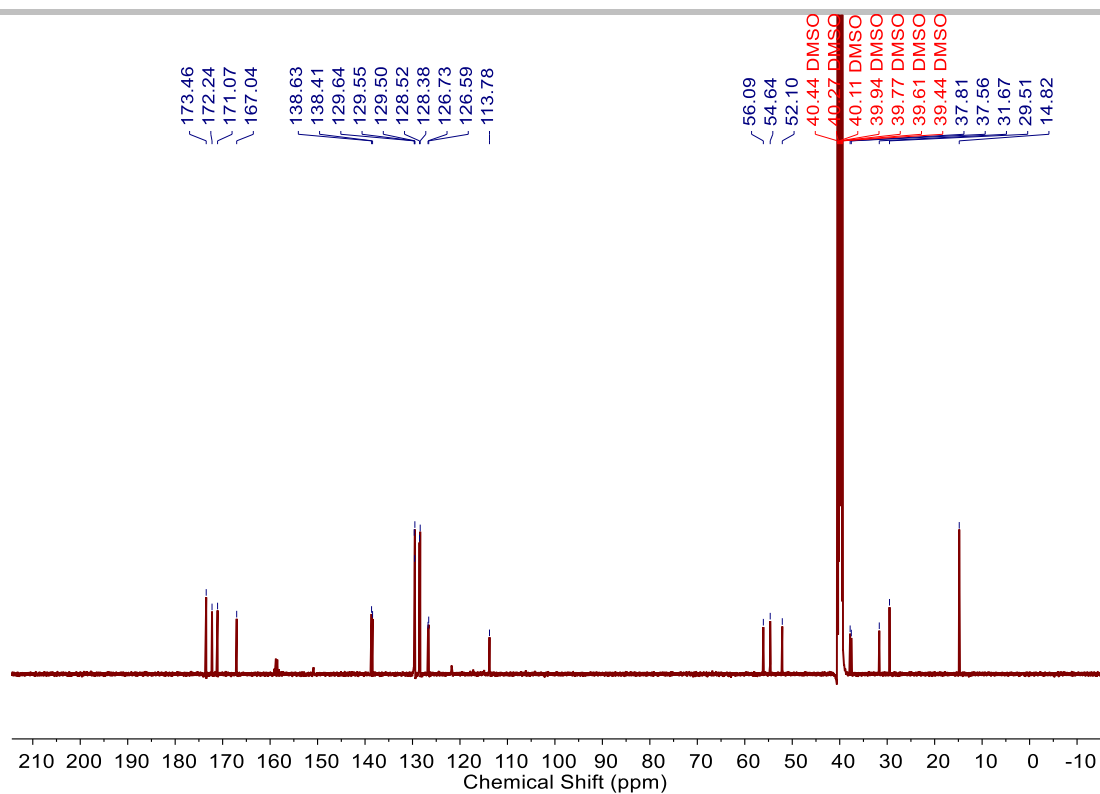


Figure S9: ^{13}C NMR spectrum (126 MHz, 298 K, $\text{DMSO-}d_6$) of the peptide D.

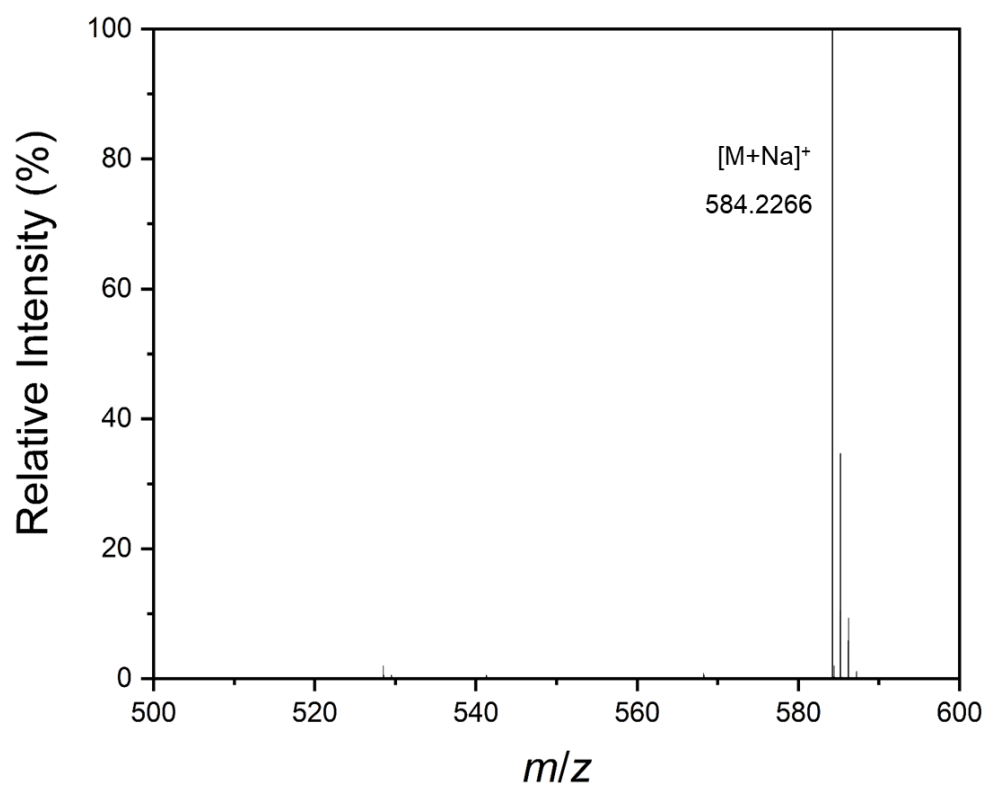
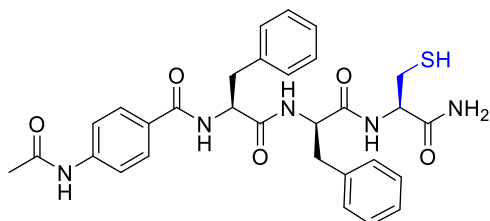


Figure S10: ESI-MS spectrum of the peptide D.

SUPPORTING INFORMATION

2.4) Peptide C analog, *N*-Ac-L-Phe-D-Phe-L-Cys-NH₂

N-Ac-L-Phe-D-Cys-L-Phe-NH₂ was synthesized following Fmoc-based SPPS under a dry and inert atmosphere. The swelling of the resin (2-chlorotrytil chloride, 0.5 g) was done in dichloromethane (5 mL). Then SOCl₂ (50 μL) was added, and the reaction was shaken under an argon flow for 1 h. After that, the resin was washed with DMF (3 × 5 mL) and dichloromethane (3 × 5 mL). Next, a solution of Fmoc-Rink amide linker (0.43 g, 0.8 mmol), DIPEA (0.45 mL) in DMF/dichloromethane

(3:2) was added to the resin, and the reaction was stirred for 3 h. Then, methanol (1 mL) was added and it was shaken for 10 minutes following by washes with DMF (3 × 5 mL) and dichloromethane (3 × 5 mL). For the deprotection, 20% piperidine in DMF (5 mL) was added to the reactor and stirred at room temperature (2 × 10 minutes). The reaction mixture was washed with DMF and dichloromethane. For the first coupling, a mixture of Fmoc-L-Cys-OH (1.05 g, 1.8 mmol), HBTU (0.46 g, 1.2 mmol), HOAt (0.16 g, 1.2 mmol) and DIPEA 1 M in DMF (1 mL) in DMF was ultrasonicated until the solution was clear, and was added to the reactor. The coupling was shaken at room temperature for 1.5 h. Then, the resin was washed and deprotected as in the previous step. The coupling and deprotection of the following amino acids (D-Cys and L-Phe) were performed using 2,4,6-trimethylpyridine 0.5 M in DMF (1 mL), by using Fmoc-D-Phe-OH (0.7 g, 1.8 mmol) for the second coupling, Fmoc-L-Phe-OH (0.7 g, 1.8 mmol) for the third one, and Fmoc-protected *p*-aminobenzoic acid for the fourth one (0.6 g, 1.8 mmol). Once deprotected the peptide was acetylated using acetic anhydride/collidine/DCM/DMF (1:1:6.7:3.3). The peptide was cleaved from the resin by shaking 2 h in the presence of a solution of TFA/DCM/H₂O/triisopropylsilane (47.5/47.5/2/3) (10 mL). The solution was drained from the reactor, and the solvent was evaporated under Ar flow. The remaining oil was dissolved in a mixture of acetonitrile/H₂O containing 0.05% TFA, followed by the precipitation of a white solid. The solid was purified by High Performance Flash Chromatography (HPFC) (Biotage® Isolera™ One 3.3.2) using Biotage® Sfär Silica HC 10g, and the following method: 3.0 Column Volume (CV) 98% DCM: 2% CH₃OH; 14.2 CV 2% to 9% of CH₃OH, 10.8 CV 9% of CH₃OH, 5.0 CV 9% to 10% of CH₃OH, 15.0 CV 10% to 12% of CH₃OH. Peptide identity was verified by ESI-MS, ¹H-NMR, and ¹³C-NMR.

¹H NMR (500 MHz, DMSO-*d*₆, 298 K) δ 10.14 (s, 1H, CONH), 8.50 (d, *J* = 8.2 Hz, 1H, CONH), 8.37 (d, *J* = 8.1 Hz, 1H, CONH), 8.27 (d, *J* = 8.3 Hz, 1H, CONH), 7.71 (d, *J* = 8.8 Hz, 2H, H_b), 7.60 (d, *J* = 8.8 Hz, 2H, H_a), 7.30 – 7.12 (m, 12H, ArH, CONH₂), 4.68 – 4.59 (m, 2H, αCH), 4.34 (td, *J* = 8.0, 5.1 Hz, 1H, αCH), 3.07 (dd, *J* = 13.6, 4.7 Hz, 1H, βCH), 2.86 – 2.66 (m, 5H, βCH), 2.05 (s, 3H, H_c).

¹³C NMR (126 MHz, DMSO-*d*₆, 298 K) δ 171.8, 171.3, 171.1, 168.7, 165.7, (5 × CO); 129.4, 129.1, 128.3, 128.1, 128.0, 127.9, 126.2, 126.1, 118.0, (Ar); 55.0, 53.8, 51.6, (αC); 40.3, 37.8, 37.1, (βC); 24.1, (CH₃).

ESI-MS: *m/z* calculated for M = 575.2202, *m/z* [M - H]⁻ 574.0

SUPPORTING INFORMATION

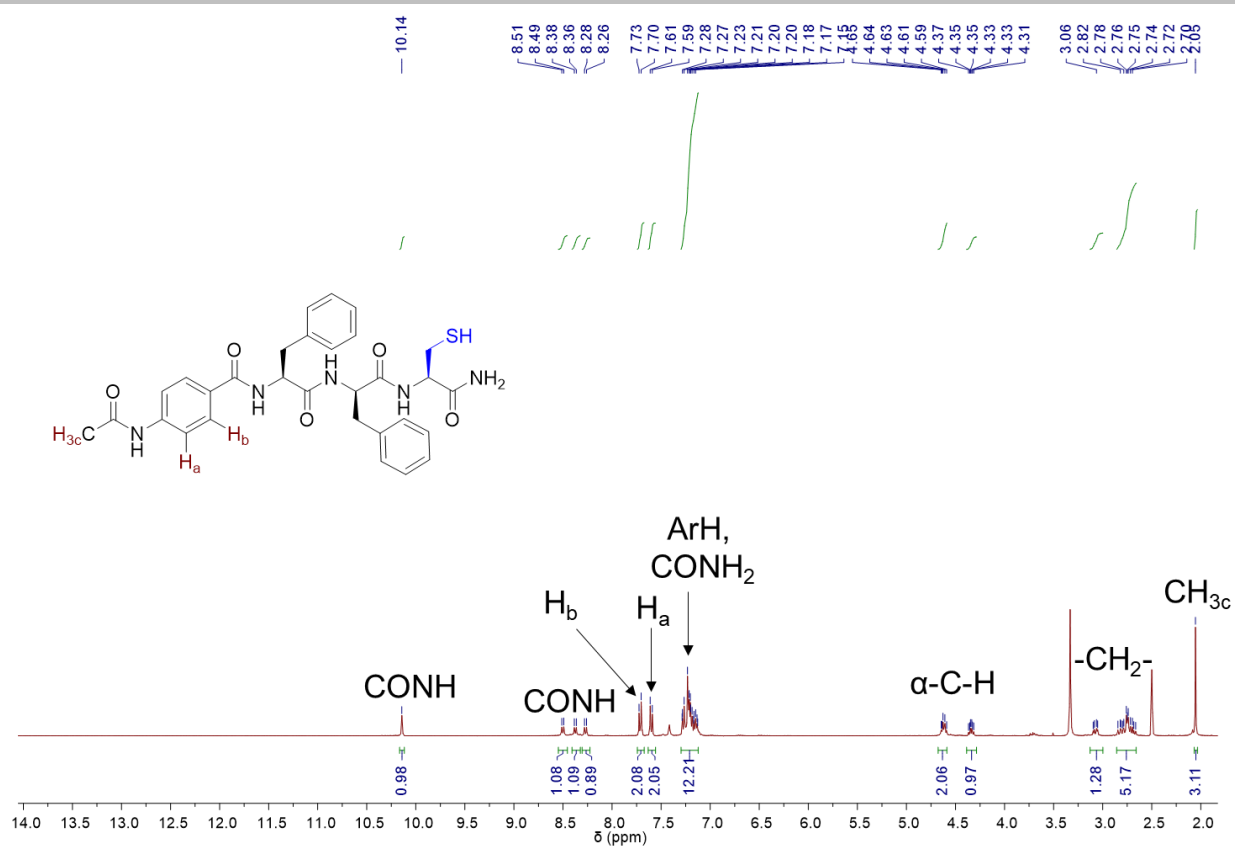


Figure S11: ¹H NMR spectrum (500 MHz, 298 K, DMSO-*d*₆) of the peptide C analog, *N*-Ac-L-Phe-D-Phe-L-Cys-NH₂.

SUPPORTING INFORMATION

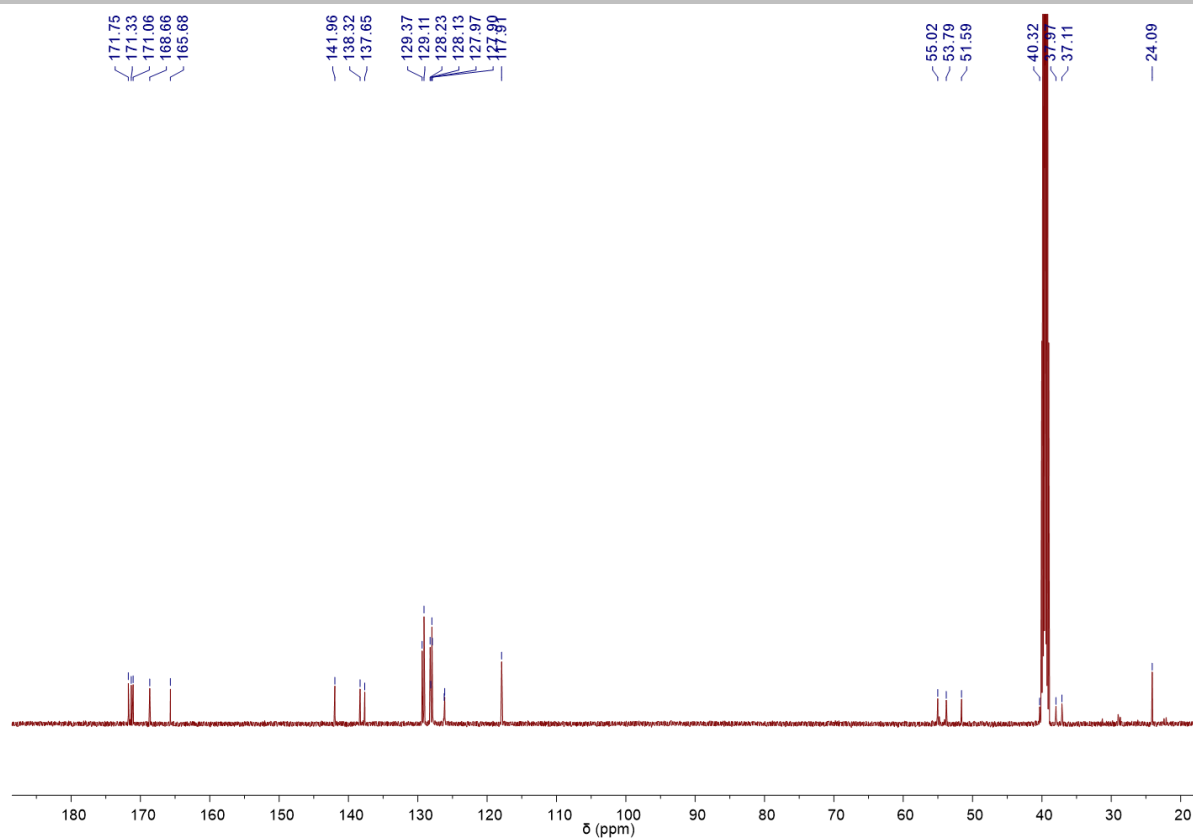


Figure S12: ^{13}C NMR spectrum (126 MHz, 298 K, $\text{DMSO-}d_6$) of the peptide **C** analog, *N*-Ac-L-Phe-D-Phe-L-Cys-NH₂.

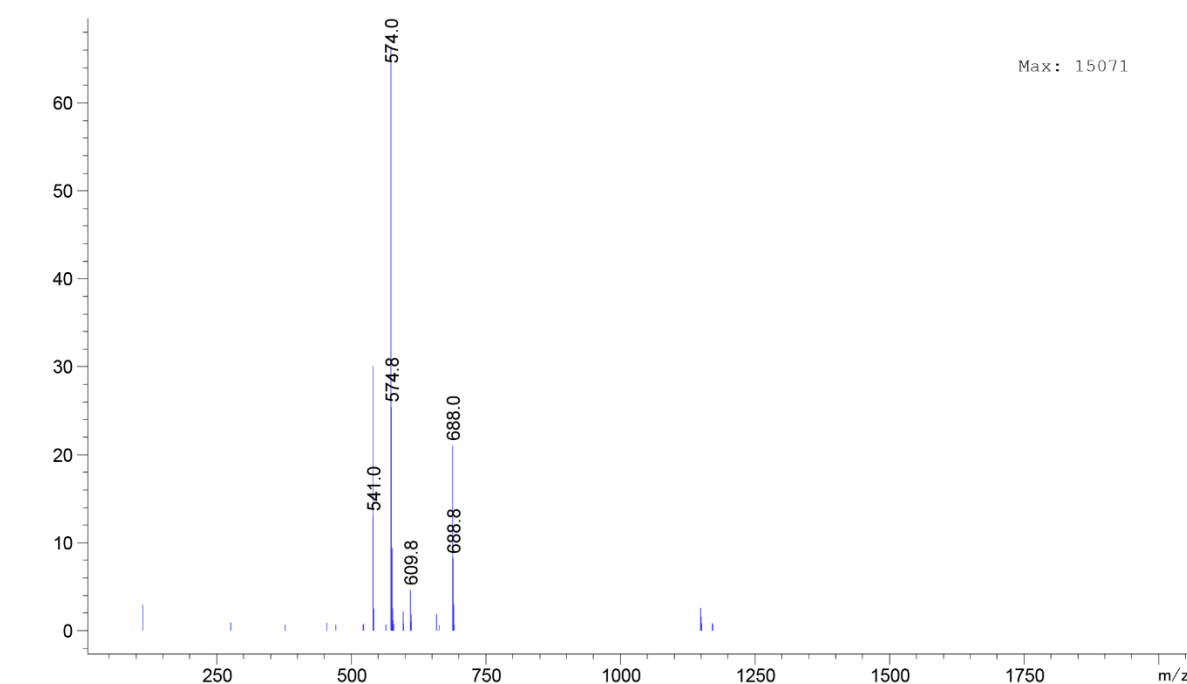
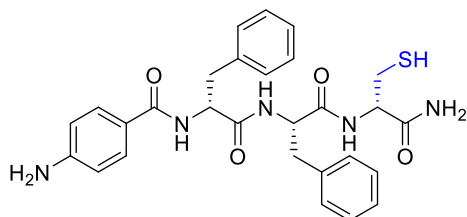


Figure S13: ESI-MS spectrum of the peptide **C** analog, *N*-Ac-L-Phe-D-Phe-L-Cys-NH₂.

SUPPORTING INFORMATION

2.5) Enantiomer of peptide C, *p*-aminobenzoyl-D-Phe-L-Phe-D-Cys-NH₂

p-Aminobenzoyl-D-Phe-L-Phe-D-Cys-NH₂ was synthesized following Fmoc-based SPPS under dry and inert atmosphere. The swelling of the resin (2-chlorotrytil chloride, 0.5 g) was done in dichloromethane (5 mL). Then SOCl₂ (0.5 μ L) was added, and the reaction was shaken under an argon flow for 1 h. After that, the resin was washed with DMF (3 \times 5 mL) and dichloromethane (3 \times 5 mL). Next, a solution of Fmoc-Rink amide linker (0.43 g, 0.8 mmol), 2,4,6-trimethylpyridine (0.90 mL) in

DMF/dichloromethane (1:1) was added to the resin, and the reaction was stirred for 1.5 h. Then methanol (1 mL) was added and it was shaken for 5 minutes followed by washes with DMF (3 \times 5 mL) and dichloromethane (3 \times 5 mL). For the deprotection, piperidine 20% in DMF (5 mL) was added to the reactor and was stirred at room temperature (2 \times 10 minutes). The reaction mixture was washed with DMF and dichloromethane. For the first coupling, a mixture of Fmoc-D-Cys-OH (1.05 g, 1.8 mmol), HBTU (0.46 g, 1.2 mmol), HOAt (0.16 g, 1.2 mmol) and 2,4,6-trimethylpyridine 0.5 M in DMF (1.2 mL) was ultrasonicated until the solution was clear, and was added to the reactor. The coupling was shaken at room temperature for 1.5 h. Then, the resin was washed and deprotected as in the previous step. The coupling and deprotection of the following amino acids (L-Phe and D-Phe) were done exactly the same way as the first coupling, by using Fmoc-L-Phe-OH (0.7 g, 1.8 mmol) for the second coupling and Fmoc-D-Phe-OH (0.7 g, 1.8 mmol) for the third one. For the introduction of *p*-aminobenzoyl motif, a coupling was performed under the same conditions by using Boc-protected *p*-aminobenzoic acid instead of a Fmoc-protected amino acid. Eventually, the peptide was cleaved from the resin by shaking 2 h in the presence of a solution of TFA/DCM/H₂O/triisopropylsilane (47.5/47.5/2/3) (10 mL). The solution was drained from the reactor, and the solvent was evaporated under air flow. The remaining oil was dissolved in a mixture of acetonitrile/H₂O (containing 0.05% of TFA), and then purified by reverse-phase HPLC (Agilent Technologies, Santa Clara, CA, USA). The HPLC Agilent 1260 Infinity system was equipped with a preparative gradient pump (1311B), semipreparative C-18 column (Kinetex, 5 microns, 100 Å , 250 mm \times 10 mm, Phenomenex, Torrance, CA, USA), autosampler (G1329B), and Photodiode Array detector (G1315C). The following HPLC method was used for the purification of the peptide: $t = 0\text{--}2$ min, 35% CH₃CN; $t = 14$ min, 65% CH₃CN; $t = 16$ min, 95% CH₃CN; $t = 17$ min, 95% CH₃CN. The compound was then freeze-dried to yield the corresponding peptide as a white fluffy powder. Peptide identity was verified by ESI-MS, ¹H-NMR, and ¹³C-NMR.

¹H NMR (500 MHz, DMSO-*d*₆, 298 K) δ 8.47 (d, $J = 8.2$ Hz, 1H, CONH), 8.13 (d, $J = 8.2$ Hz, 1H, CONH), 8.04 (d, $J = 7.8$ Hz, 1H, CONH), 7.49 (d, $J = 8.7$ Hz, 2H, H_b), 7.31 – 7.06 (m, 12H, ArH, CONH₂), 6.52 (d, $J = 8.6$ Hz, 2H, H_a), 4.55 (m, 2H, α H), 4.31 (td, $J = 7.9, 5.0$ Hz, 1H, α H), 3.09 (dd, $J = 13.8, 4.0$ Hz, 1H, β H), 2.87 – 2.66 (m, 5H, β H), 2.28 (t, $J = 8.4$ Hz, 1H, SH).

¹³C NMR (126 MHz, DMSO-*d*₆, 298 K) δ 172.2, 171.3, 171.1, 168.5, (4 \times CO); 151.1, 138.4, 137.8, 129.3, 129.1, 129.0, 128.0, 127.9, 126.2, 126.1, 120.9, 112.8, (Ar); 56.1, 54.0, (3 \times α C); 37.2, 36.9, 26.0, (3 \times β C).

ESI-MS: m/z calculated for M = 533.2097, observed positive mode [M + H]⁺ = 534.0.

SUPPORTING INFORMATION

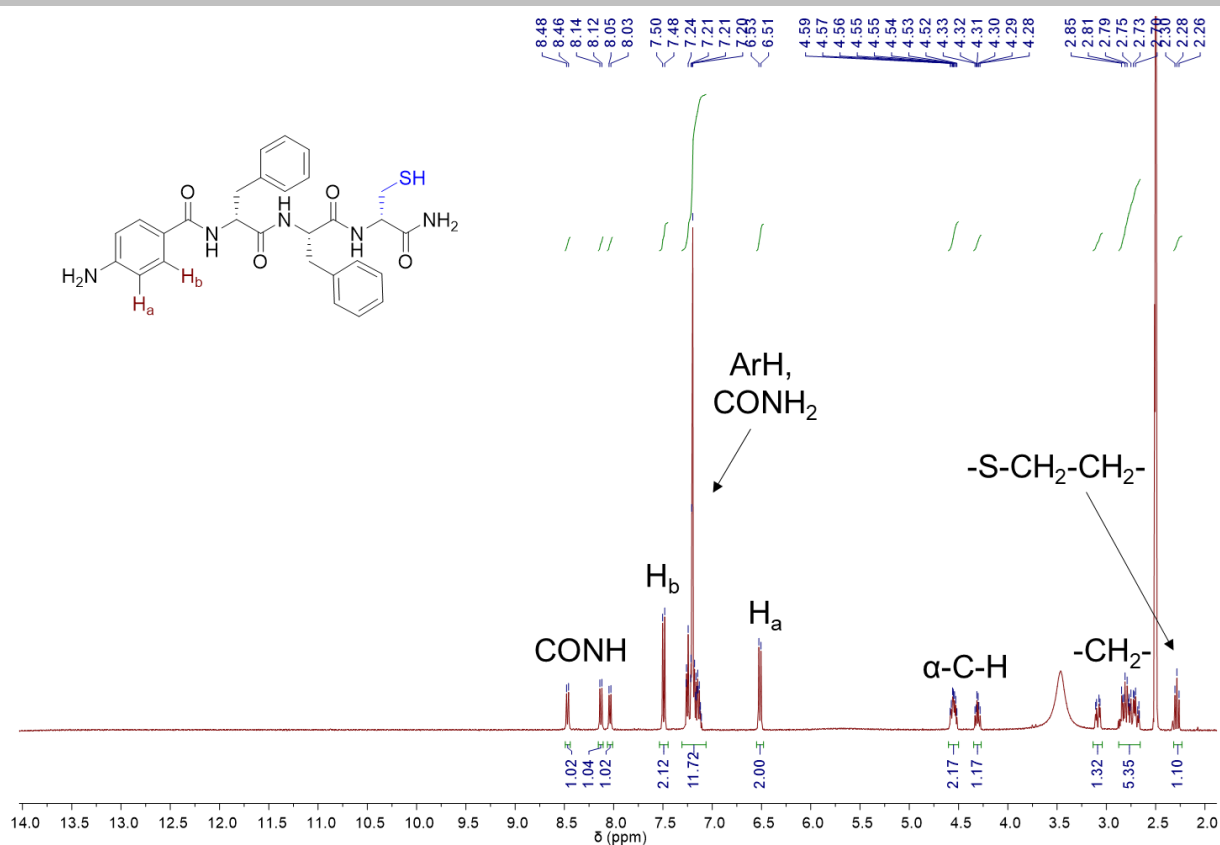


Figure S14: ¹H NMR spectrum (500 MHz, 298 K, DMSO-*d*₆) of the enantiomer of peptide C, *p*-aminobenzoyl-D-Phe-L-Phe-D-Cys-NH₂.

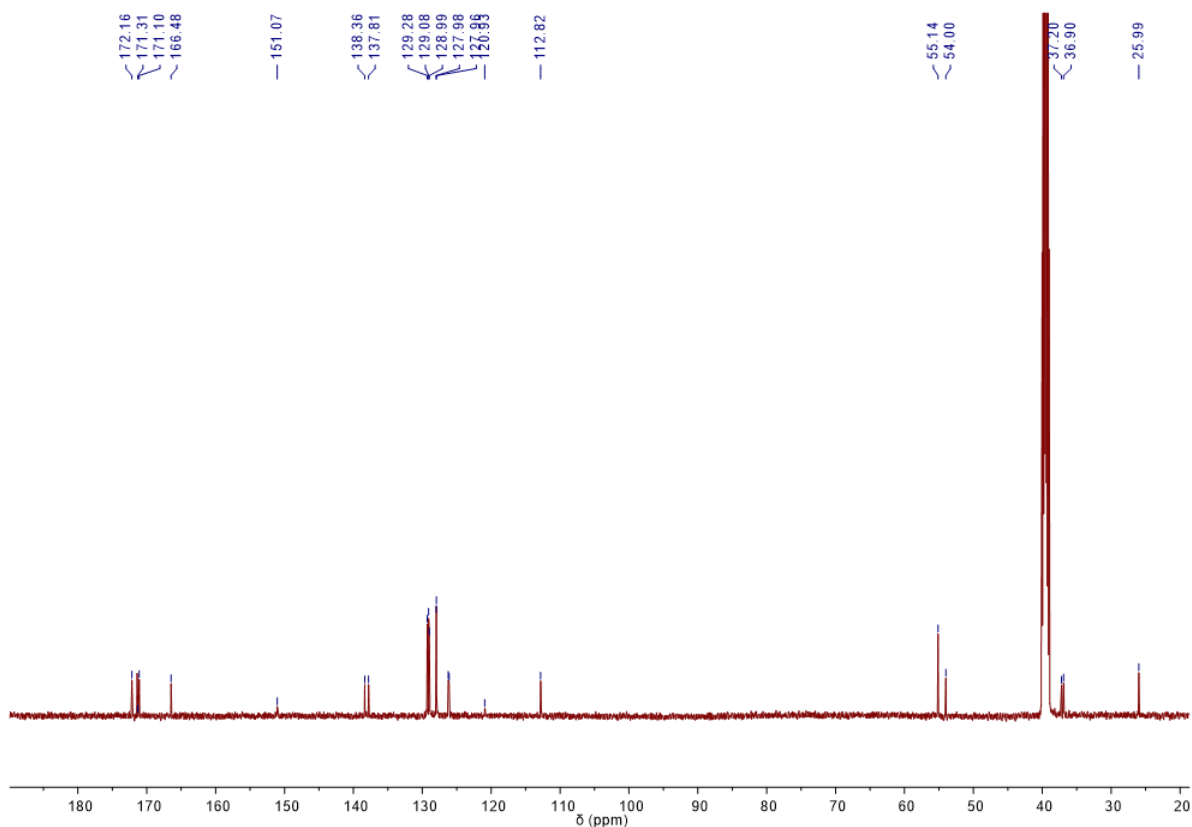


Figure S15: ¹³C NMR spectrum (126 MHz, 298 K, DMSO-*d*₆) of the enantiomer of peptide C, *p*-aminobenzoyl-D-Phe-L-Phe-D-Cys-NH₂.

SUPPORTING INFORMATION

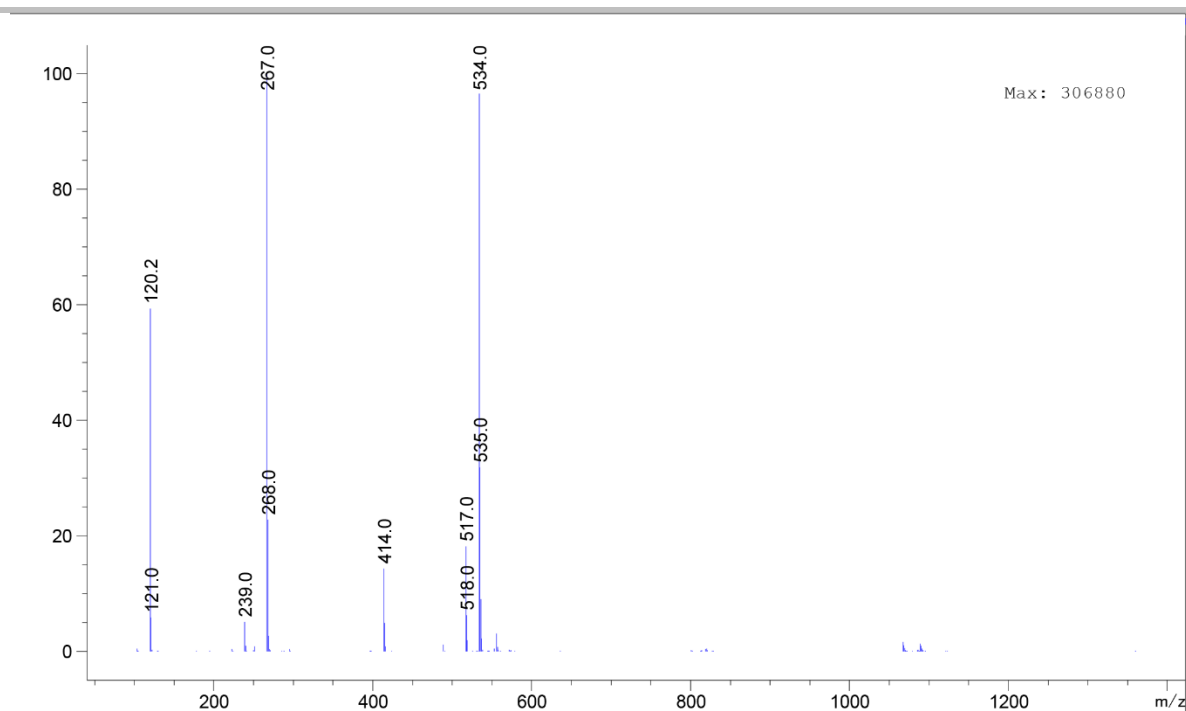
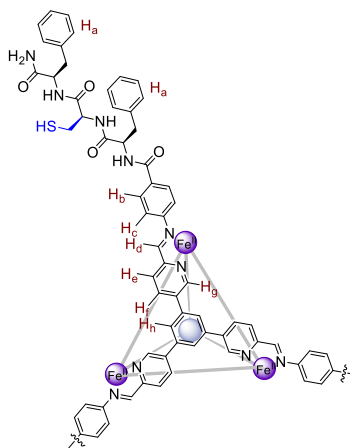


Figure S16: ESI-MS spectrum of the enantiomer of peptide **C**, *p*-aminobenzoyl-D-Phe-L-Phe-D-Cys-NH₂.

2.6) Cage 1



A (3.0 mg, 0.0076 mmol, 1.0 equiv) and **B** (12.2 mg, 0.0229 mmol, 3.0 equiv) were dissolved in 3.0 mL of CH₃CN in a sealed 10 mL round bottom flask. The solution was degassed with N₂ for 10 min, after which Fe(NTf₂)₂ (5.31 mg, 0.0076 mmol, 1.0 equiv) was added. The solution was degassed for an additional 10 min. The solution was heated at 70 °C for 18 h. The solution was then cooled and concentrated under a flow of nitrogen. Addition of 10 mL of diethyl ether precipitated the product as a dark purple solid. The solid was separated by centrifugation and washed with diethyl ether (2 × 10 mL), then dried under a flow of N₂ with yield of 90%.

This compound exhibited poor solubility in CD₃CN that is not sufficient for ¹³C NMR spectrum. Only ¹H and ¹⁹F NMR spectra are presented.

¹⁹F NMR (471 MHz, 298 K, CD₃CN) δ -79.29 (encapsulated TFA⁻), -80.02 (free NTf₂⁻).

HR-MS: *m/z*, 2234.3305 [1(NTf₂)₃(CF₃COO)⁴⁺, 2234.4917], 1731.4757 [1(NTf₂)₂(CF₃COO)⁵⁺, 1731.5636], 1396.2436 [1(NTf₂)(CF₃COO)⁶⁺, 1396.2782], 1156.6459 [1(CF₃COO)⁷⁺, 1156.7886].

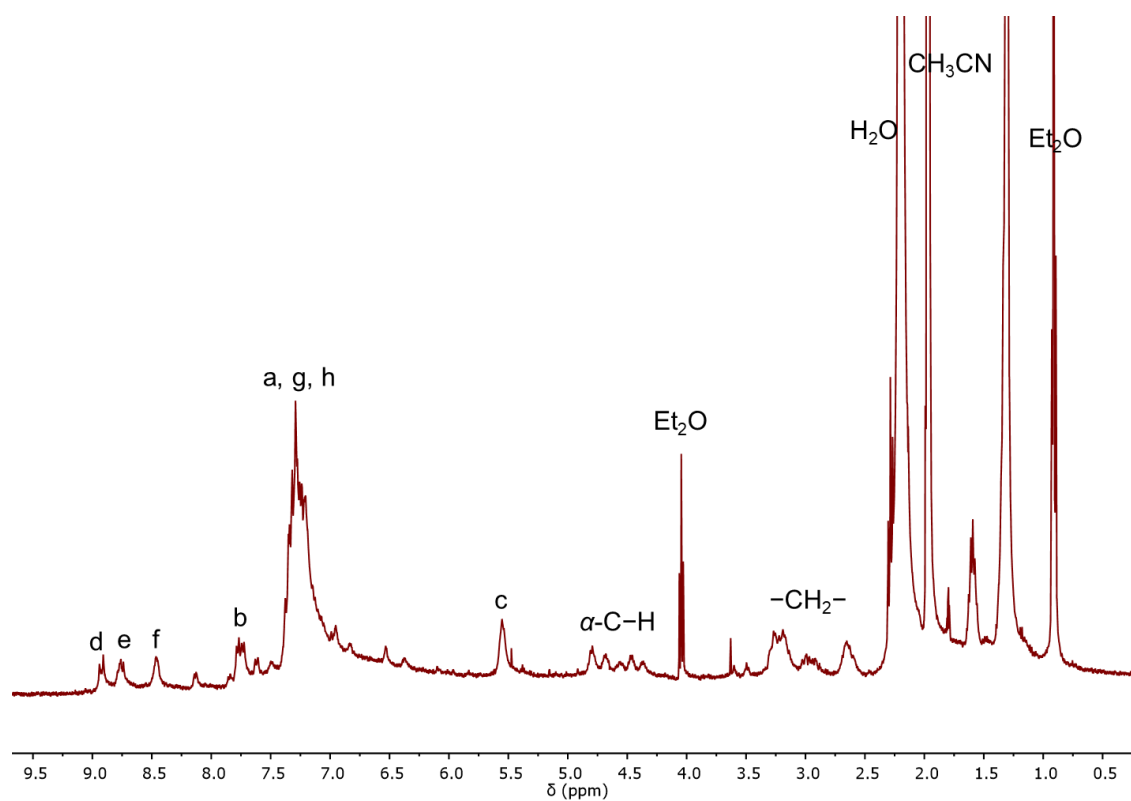


Figure S17: ^1H NMR spectrum (400 MHz, 298 K, CD_3CN) of **1**.

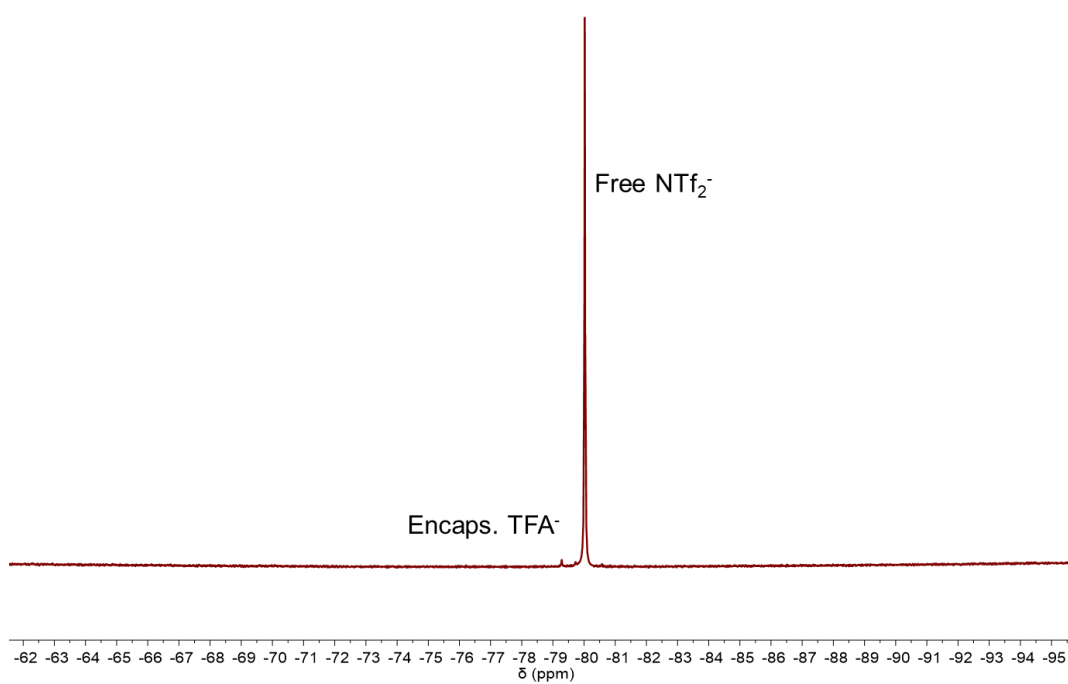


Figure S18: ^{19}F NMR spectrum (471 MHz, 298 K, CD_3CN) of **1**.

SUPPORTING INFORMATION

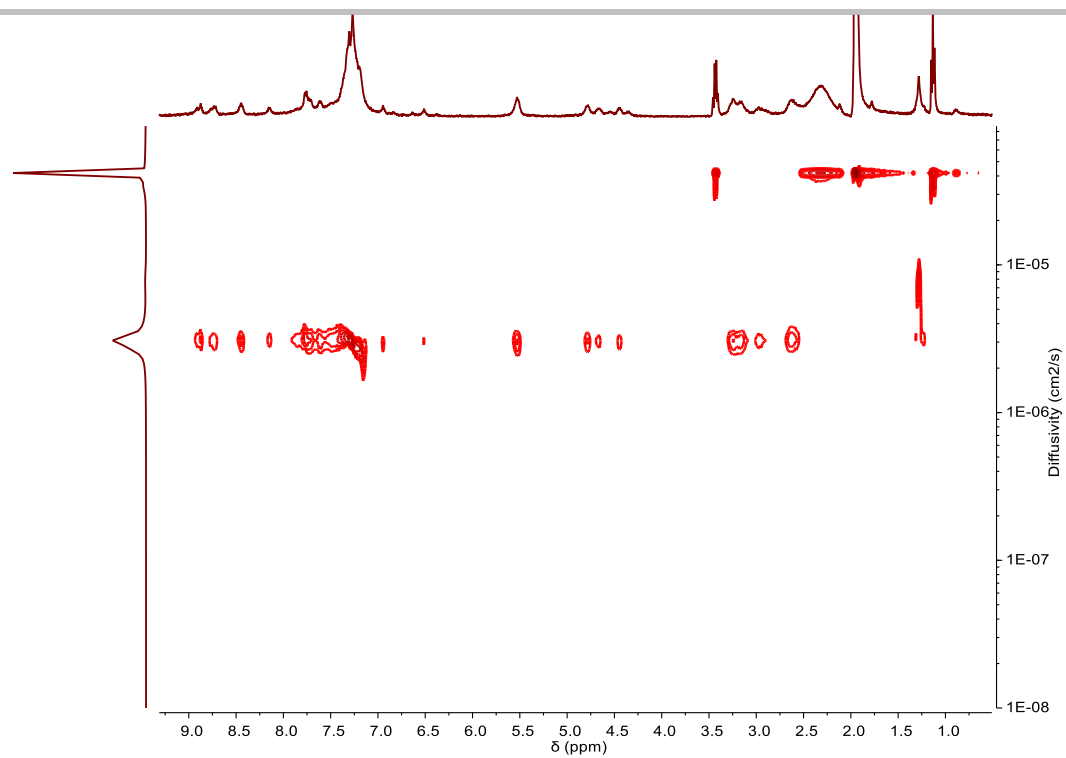


Figure S19: ¹H DOSY spectrum (400 MHz, 298 K, CD₃CN) of **1**. The diffusion coefficient in CD₃CN was measured to be $3.01 \times 10^{-6} \text{ cm}^2/\text{s}$, $R = 21.7 \text{ \AA}$.

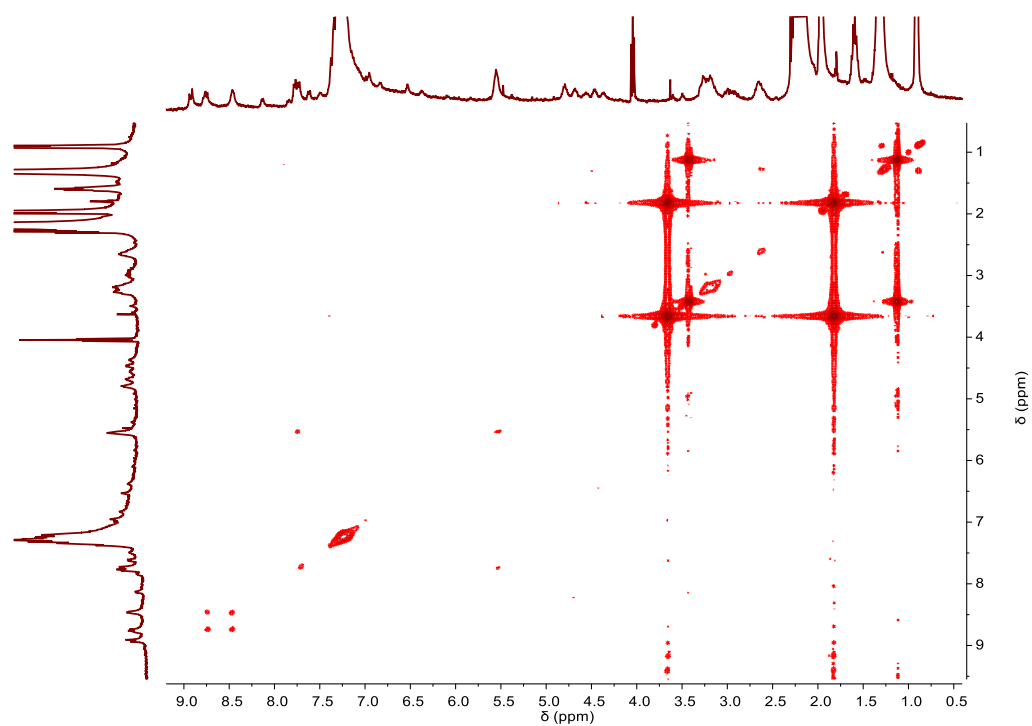


Figure S20: ¹H-¹H COSY NMR spectrum (500 MHz, 298 K, CD₃CN) of **1**.

SUPPORTING INFORMATION

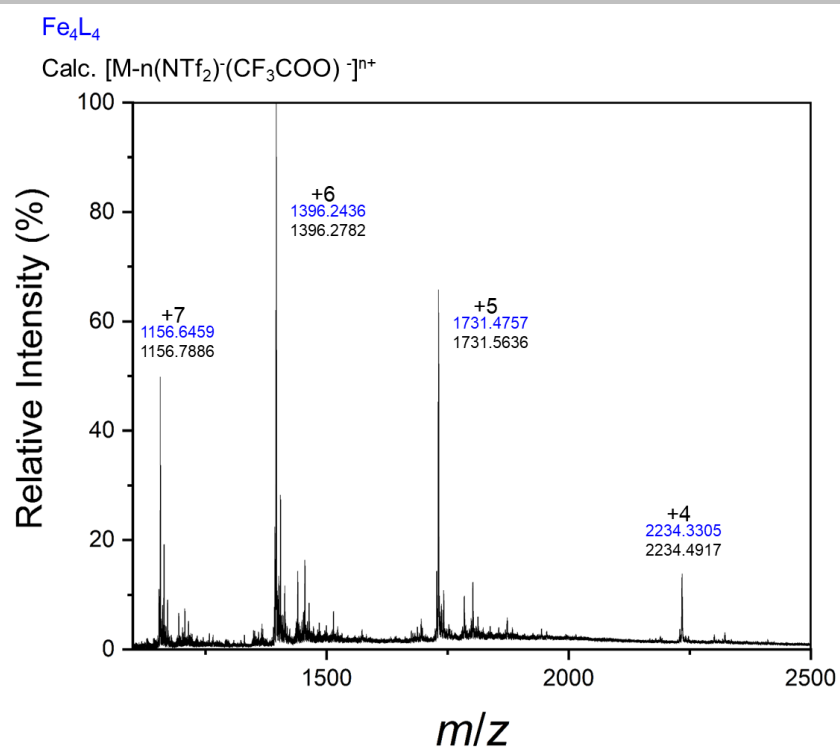


Figure S21: High-resolution ESI-MS spectrum of **1** in CH_3CN . Experimental (blue) and calculated (black) peaks.

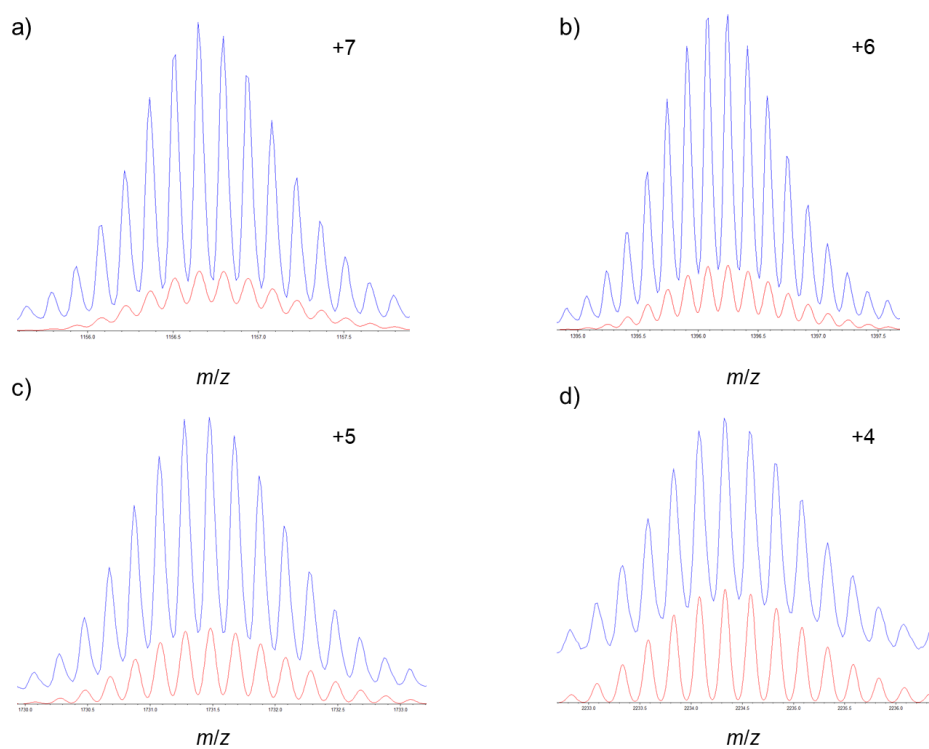
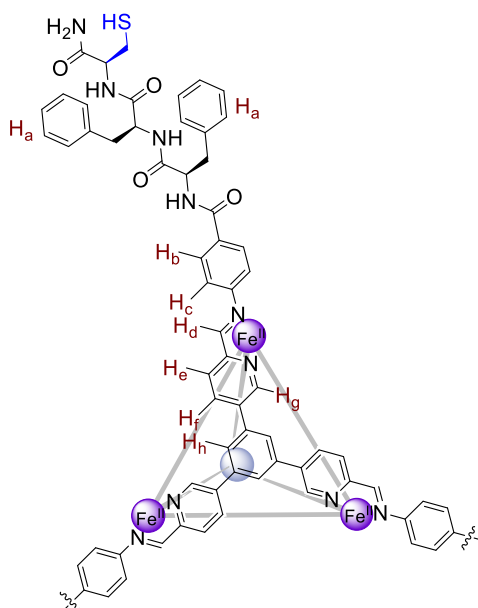


Figure S22: High-resolution ESI-MS spectra of **1** in CH_3CN . Experimental (blue) and calculated (red) peaks for a) $[\mathbf{1}(\text{CF}_3\text{COO})]^{7+}$ b) $[\mathbf{1}(\text{NTf}_2)(\text{CF}_3\text{COO})]^{6+}$ c) $[\mathbf{1}(\text{NTf}_2)_2(\text{CF}_3\text{COO})]^{5+}$ d) $[\mathbf{1}(\text{NTf}_2)_3(\text{CF}_3\text{COO})]^{4+}$.

SUPPORTING INFORMATION

2.7) Cage 2



C (12.2 mg, 0.0229 mmol, 3.0 equiv) and **A** (3.0 mg, 0.0076 mmol, 1.0 equiv) were dissolved in 3.0 mL of CH_3CN in a sealed 10 mL round bottom flask. The solution was degassed with N_2 for 10 min, after which $\text{Fe}(\text{NTf}_2)_2$ (5.31 mg, 0.0076 mmol, 1.0 equiv.) was added. The solution was degassed for an additional 10 min. The solution was heated at 70°C for 18 h. The dark purple solution was then cooled and concentrated under a flow of nitrogen. Addition of 10 mL of diethyl ether precipitated the compound into a dark purple solid. The solid was separated by centrifugation and washed with diethyl ether ($2 \times 10\text{ mL}$), then dried under a flow of nitrogen with yield of 90%.

This compound has poor solubility in CD_3CN that is not sufficient for ^{13}C NMR spectrum. Only ^1H and ^{19}F NMR spectra are presented. ^{19}F NMR (471 MHz, acetonitrile- d_3) δ -76.24 (free TFA $^-$), -79.29 (encapsulated TFA $^-$), -80.06 (NTf_2^-).

HRMS [charge, calculated mass]: $m/z = 2234.3234$ [$2(\text{NTf}_2)_3(\text{CF}_3\text{COO})^{4+}$, 2234.4917], 1731.4730 [$2(\text{NTf}_2)_2(\text{CF}_3\text{COO})^{5+}$, 1731.5636], 1396.2428 [$2(\text{NTf}_2)(\text{CF}_3\text{COO})^{6+}$, 1396.2782], 1156.7926 [$2(\text{CF}_3\text{COO})^{7+}$, 1156.7886].

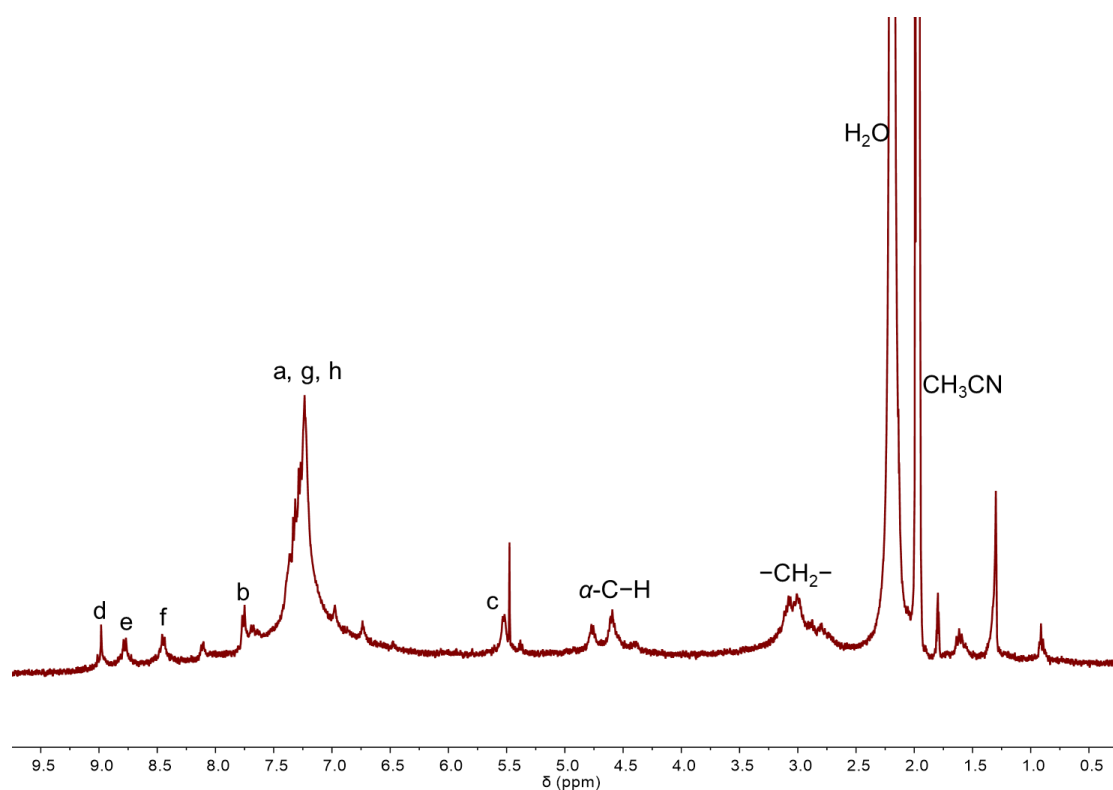


Figure S23: ^1H NMR spectrum (400 MHz, 298 K, CD_3CN) of **2**.

SUPPORTING INFORMATION

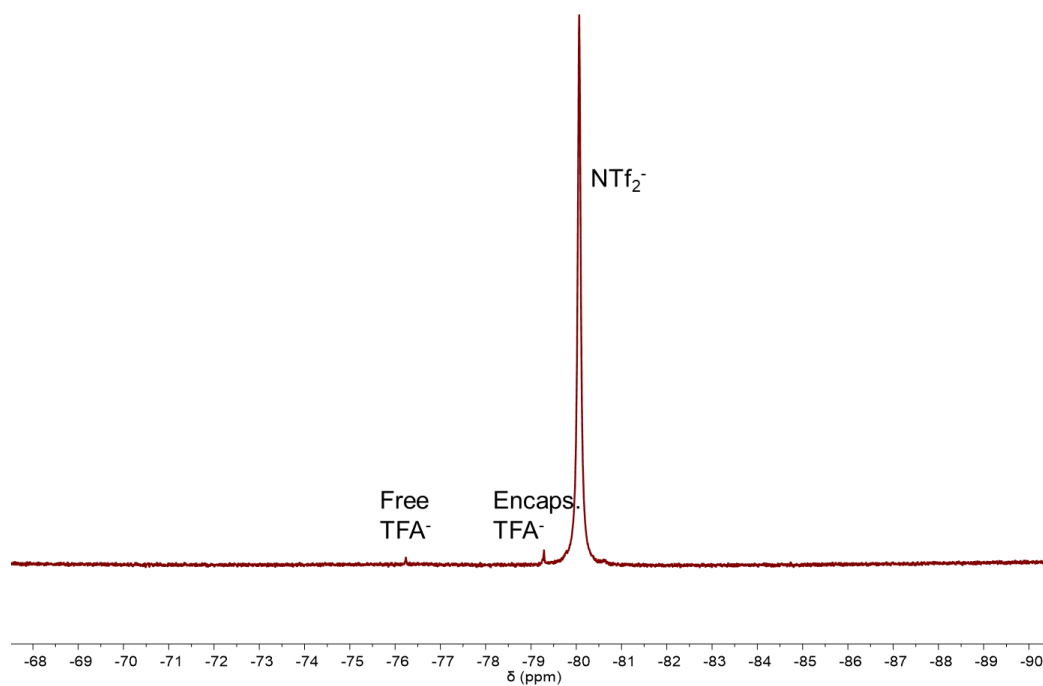


Figure S24: ^{19}F NMR spectrum (471 MHz, 298 K, CD_3CN) of **2**.

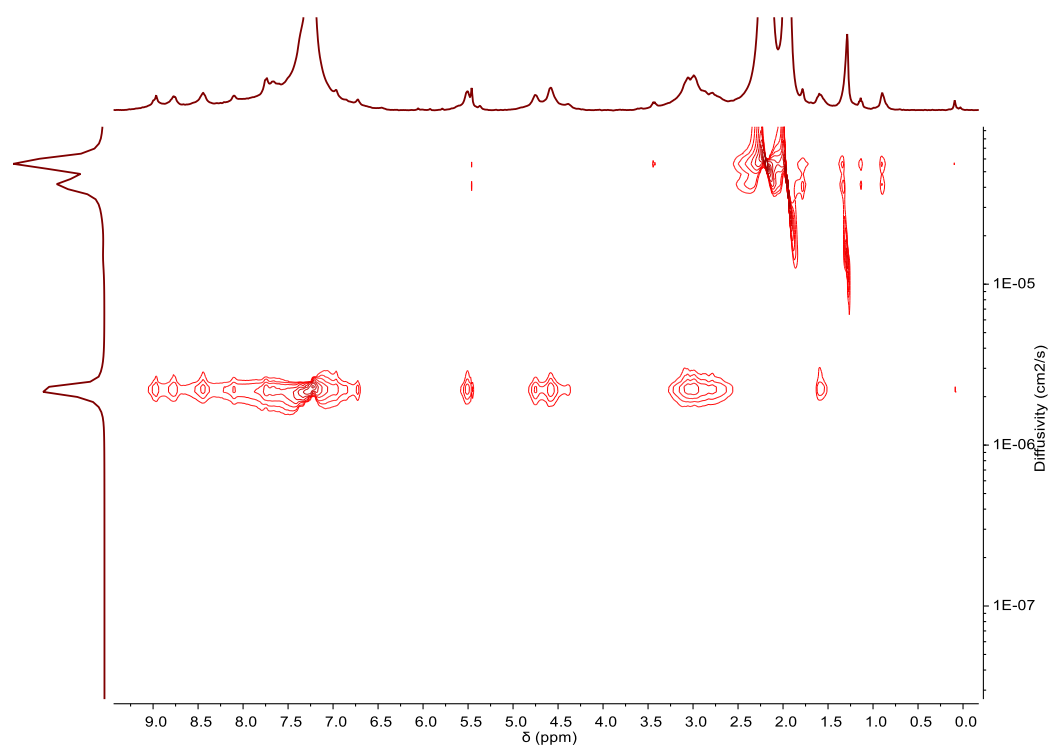


Figure S25: ^1H DOSY spectrum (400 MHz, 298 K, CD_3CN) of **2**. The diffusion coefficient in CD_3CN was measured to be $2.14 \times 10^{-6} \text{ cm}^2/\text{s}$, $R = 30.5 \text{ \AA}$.

SUPPORTING INFORMATION

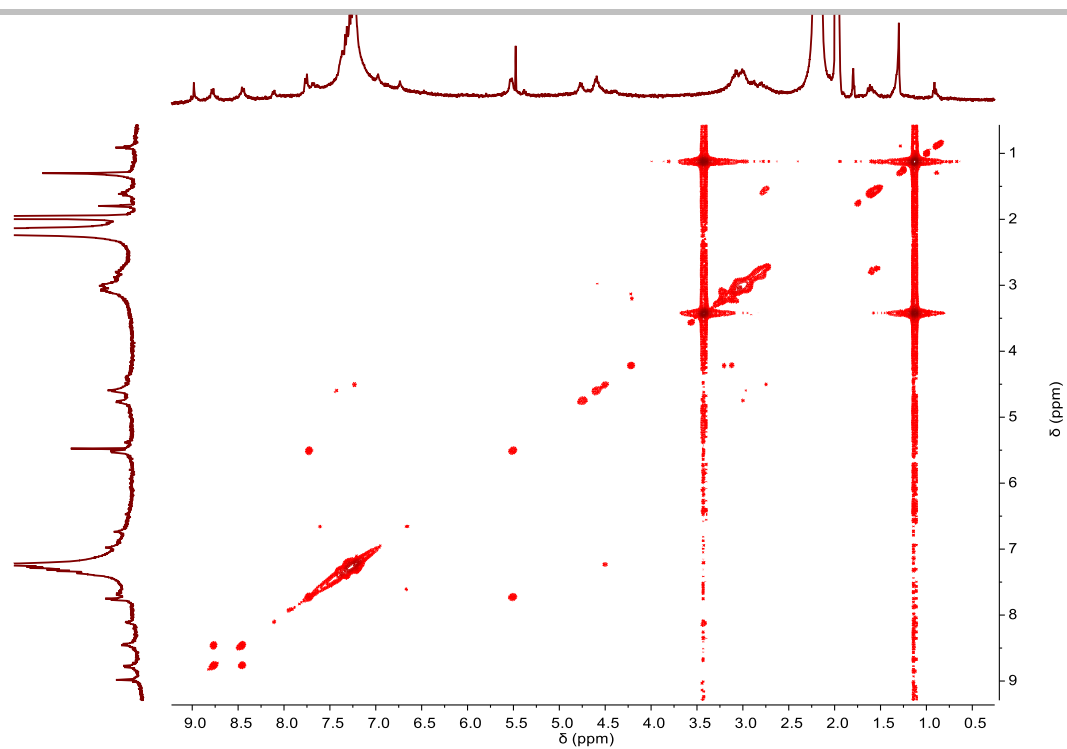


Figure S26: ^1H - ^1H COSY spectrum (500 MHz, 298 K, CD_3CN) of **2**.

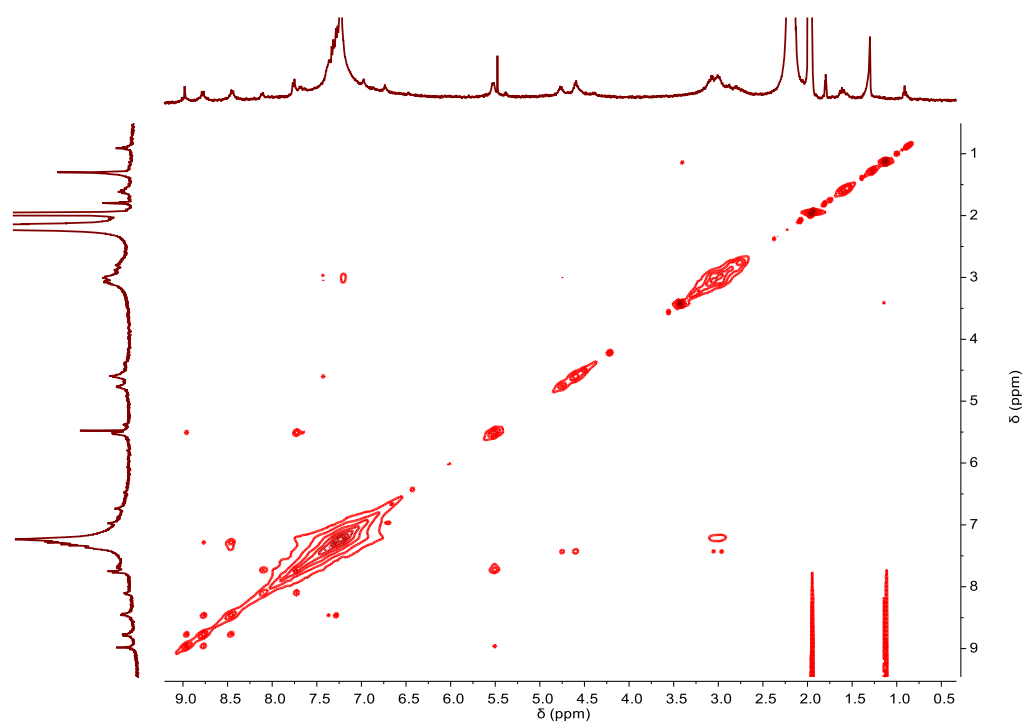


Figure S27: NOESY spectrum (500 MHz, 298 K, CD_3CN) of **2**.

SUPPORTING INFORMATION

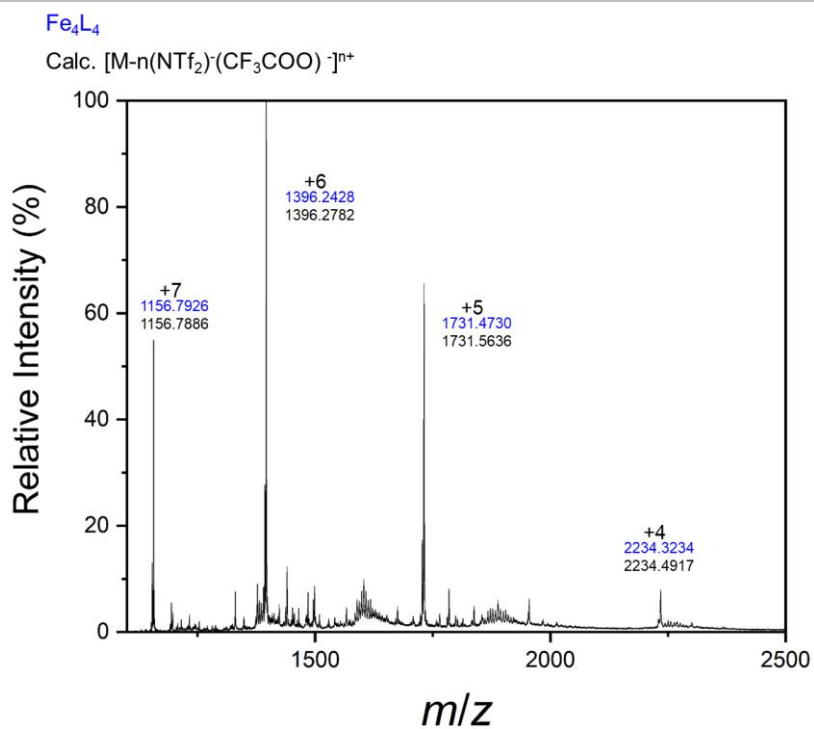


Figure S28: High-resolution ESI-MS spectrum of **2** in CH_3CN . Experimental (blue) and calculated (black) peaks.

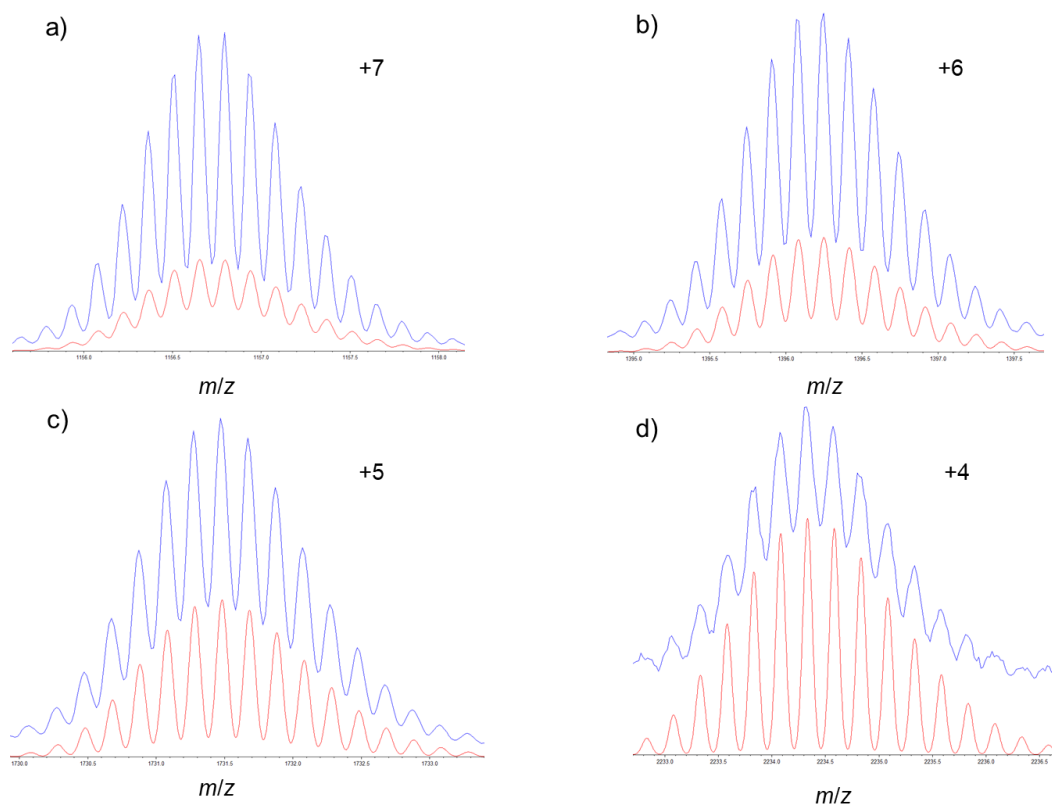
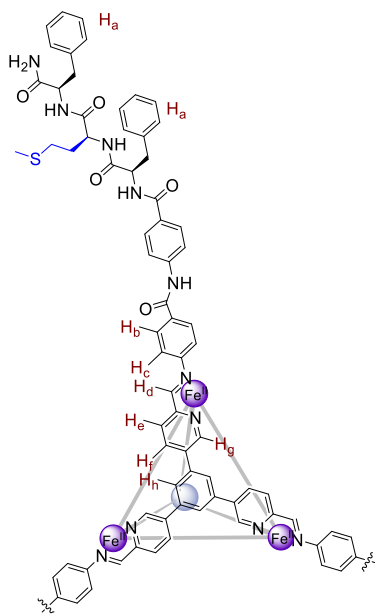


Figure S29: High-resolution ESI-MS spectra of **2** in CH_3CN . Experimental (blue) and calculated (red) peaks for a) $[\text{2}(\text{CF}_3\text{COO})]^{7+}$, b) $[\text{2}(\text{NTf}_2)(\text{CF}_3\text{COO})]^{6+}$, c) $[\text{2}(\text{NTf}_2)_2(\text{CF}_3\text{COO})]^{5+}$, and d) $[\text{2}(\text{NTf}_2)_3(\text{CF}_3\text{COO})]^{4+}$.

SUPPORTING INFORMATION

2.8) Cage 3



D (12.8 mg, 0.0229 mmol, 3.0 equiv.) and **A** (3.0 mg, 0.0076 mmol, 1.0 equiv.) were dissolved in 3.0 mL of CH₃CN in a sealed 10 mL round bottom flask. The solution was degassed with N₂ for 10 min, after which Fe(NTf₂)₂ (5.31 mg, 0.0076 mmol, 1.0 equiv.) was added. The solution was degassed for an additional 10 min. The solution was heated at 70 °C for 18 h. The dark purple solution was then cooled and concentrated under a flow of nitrogen. Addition of 10 mL of diethyl ether precipitated the compound as a dark purple solid. The solid was separated by centrifugation and washed with diethyl ether (2 × 10 mL), then dried under a flow of nitrogen with a yield of 90%.

¹⁹F NMR (471 MHz, acetonitrile-*d*₃) δ -76.22 (free TFA⁻), -79.27 (encapsulated TFA⁻), -80.05 (NTf₂⁻).

HR-MS [charge, calculated mass]: *m/z* = 2318.6884 [**3**(NTf₂)₃(CF₃COO)⁴⁺, 2318.6514], 1798.7642 [**3**(NTf₂)₂(CF₃COO)⁵⁺, 1798.8913], 1452.3153 [**3**(NTf₂)(CF₃COO)⁶⁺, 1452.3846], 1204.8519 [**3**(CF₃COO)⁷⁺, 1204.8798].

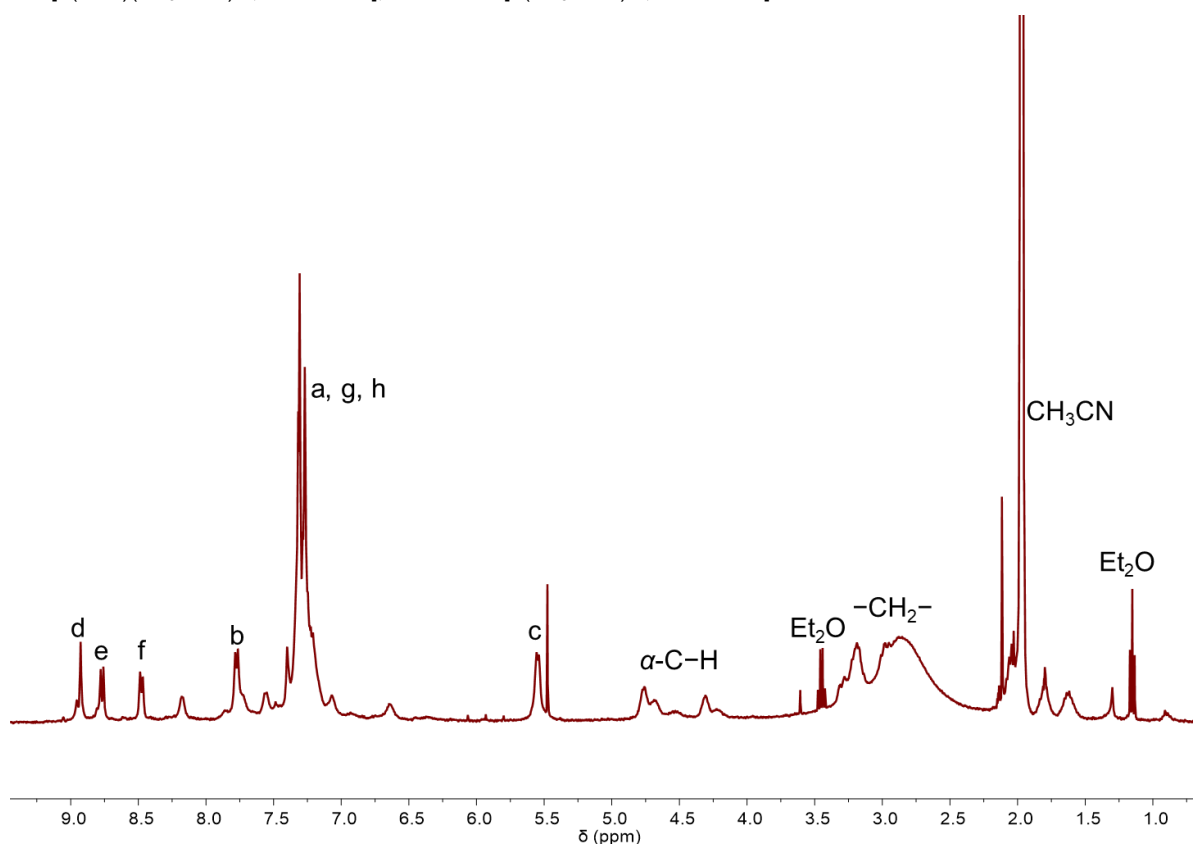


Figure S30: ¹H NMR spectrum (400 MHz, 298 K, CD₃CN) of **3**.

SUPPORTING INFORMATION

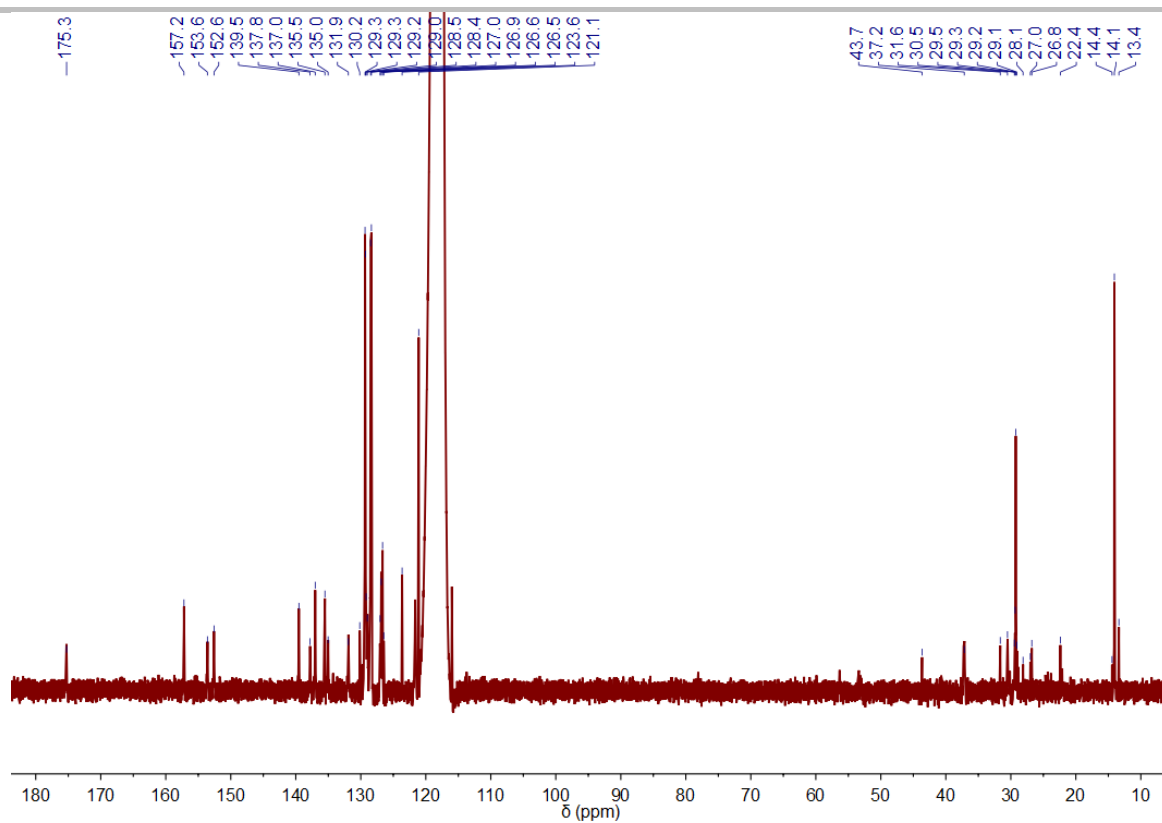


Figure S31: ^{13}C NMR spectrum (126 MHz, 298 K, CD_3CN) of **3**.

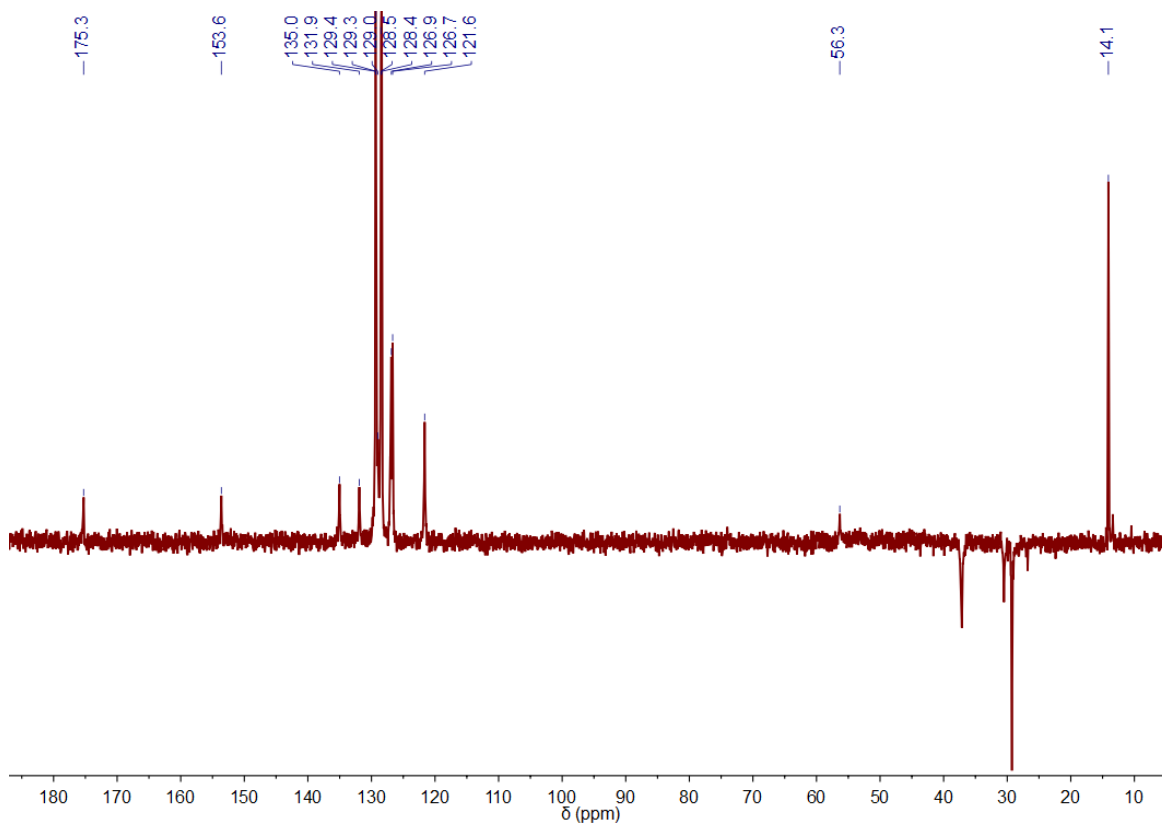


Figure S32: ^{13}C NMR dept (126 MHz, CD_3CN) of **3**.

SUPPORTING INFORMATION

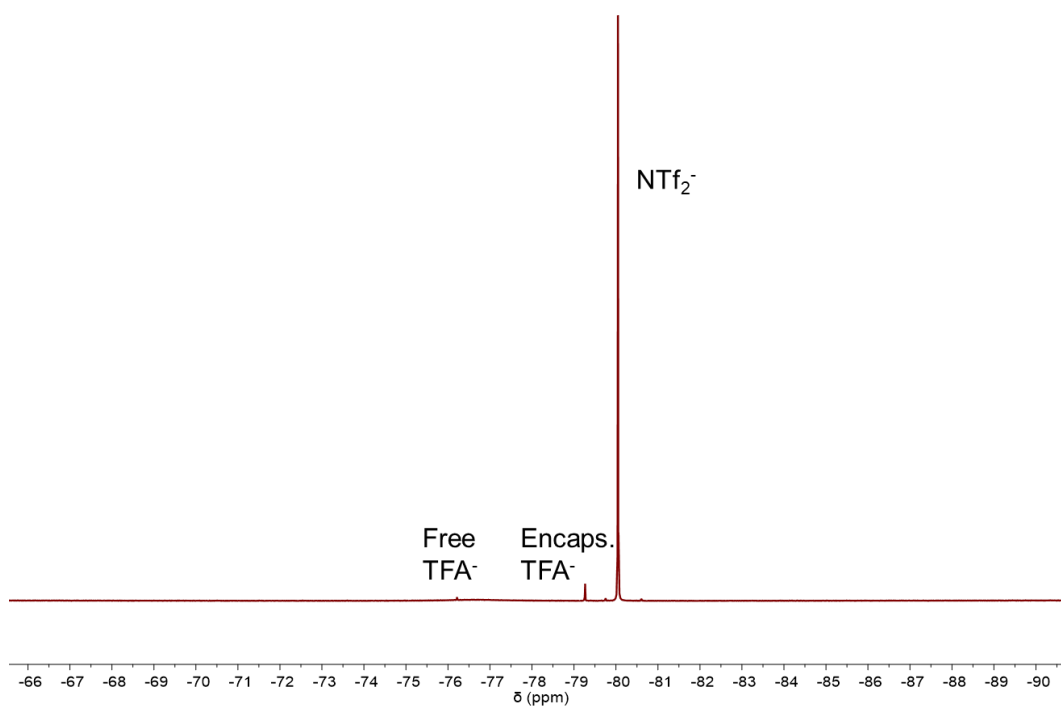


Figure S33: ¹⁹F NMR spectrum (471 MHz, 298 K, CD₃CN) of **3**.

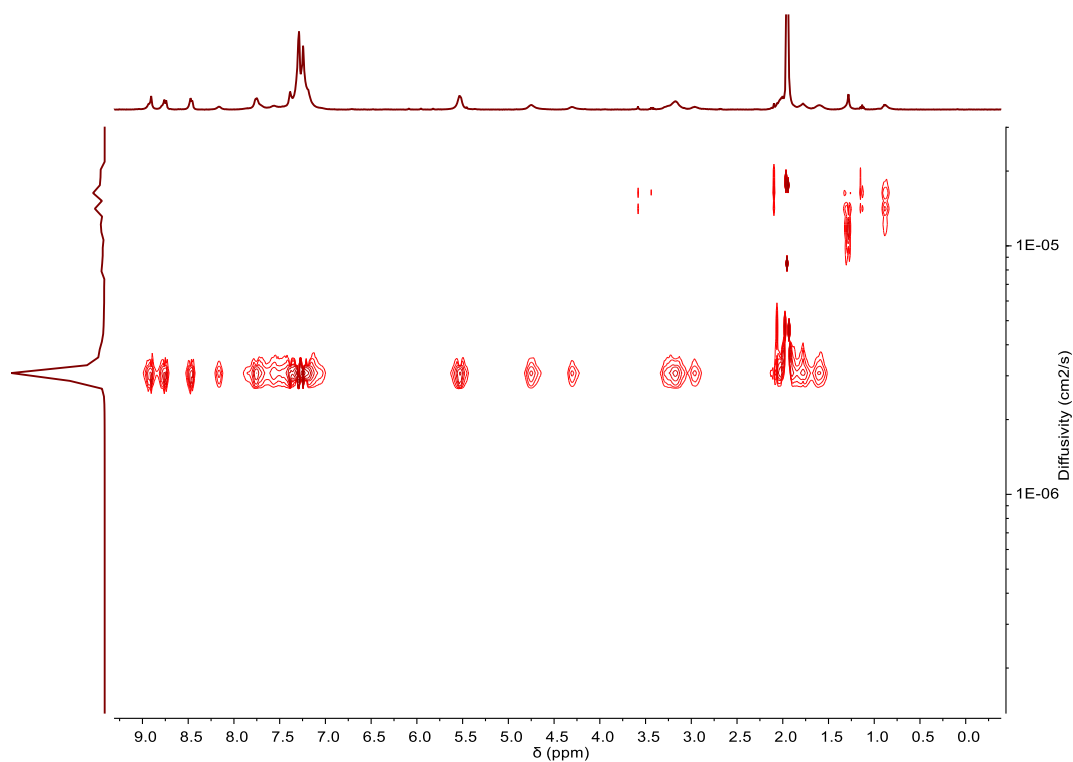


Figure S34: ¹H DOSY spectrum (400 MHz, 298 K, CD₃CN) of **3**. The diffusion coefficient in CD₃CN was measured to be 3.07×10^{-6} cm²/s, $R = 21.3$ Å.

SUPPORTING INFORMATION

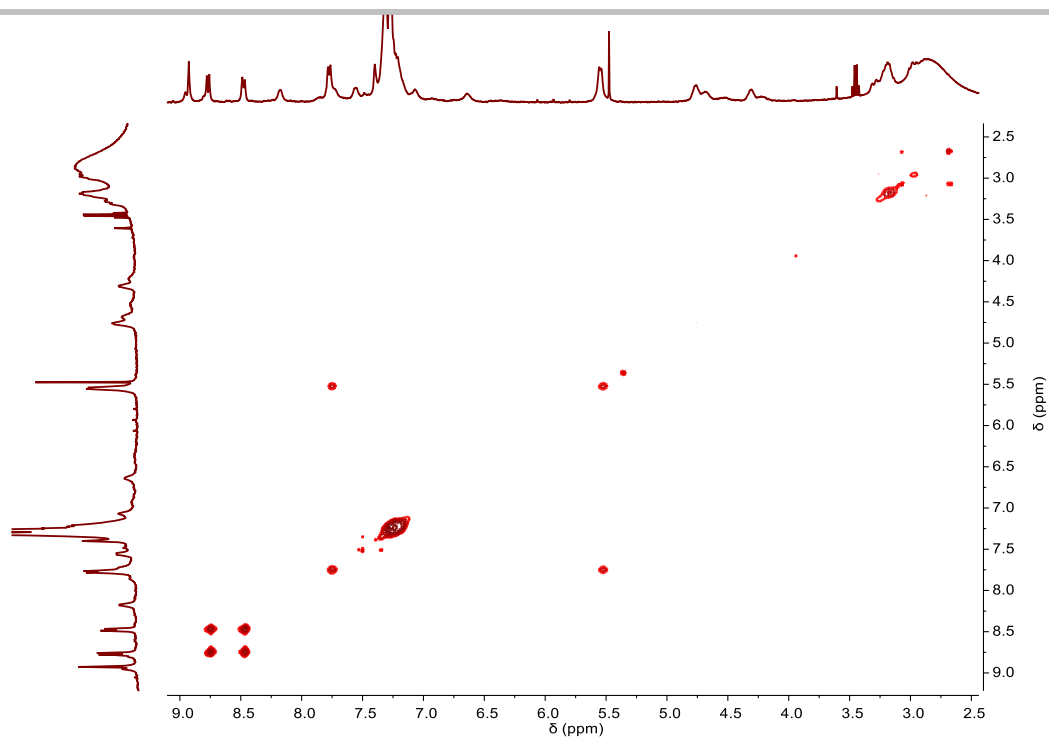


Figure S35: ¹H-¹H COSY spectrum (400 MHz, 298 K, CD₃CN) of **3**.

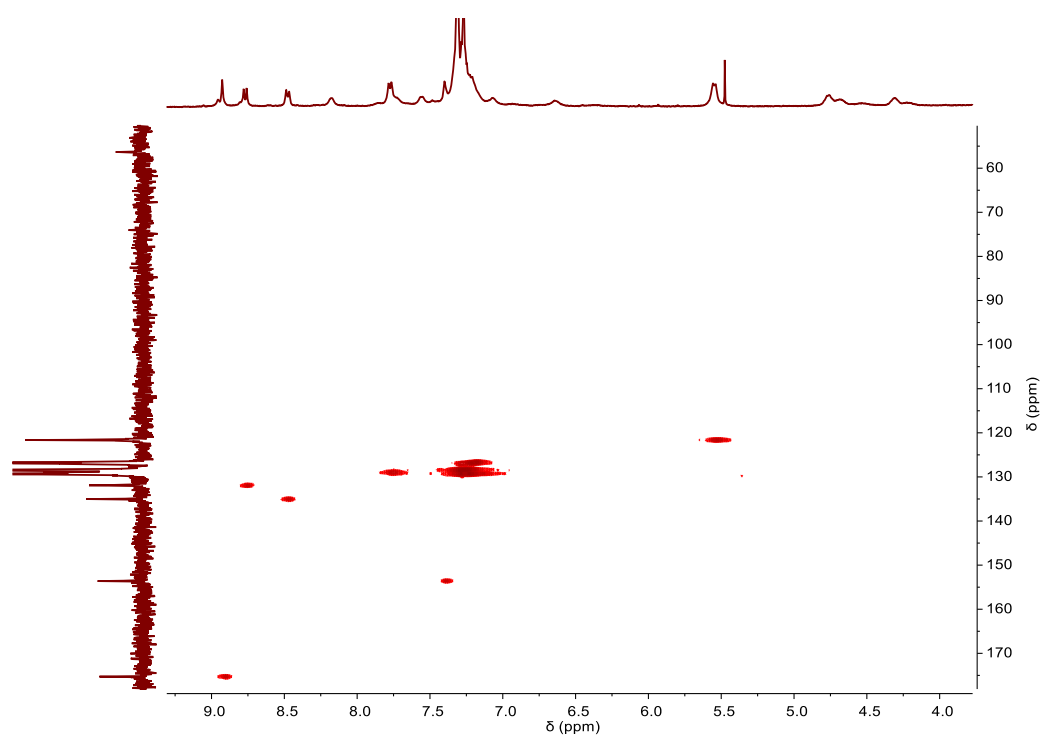


Figure S36: HSQC spectrum (500 MHz, 298 K, CD₃CN) of **3**.

SUPPORTING INFORMATION

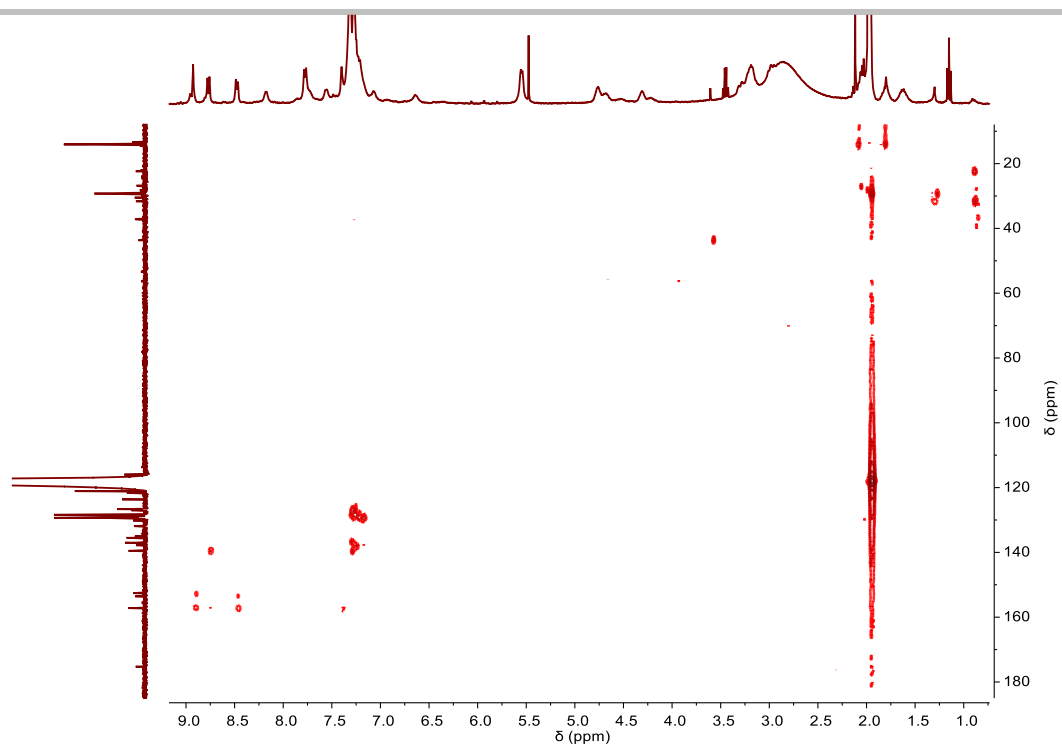


Figure S37: HMBC spectrum (500 MHz, 298 K, CD₃CN) of **3**.

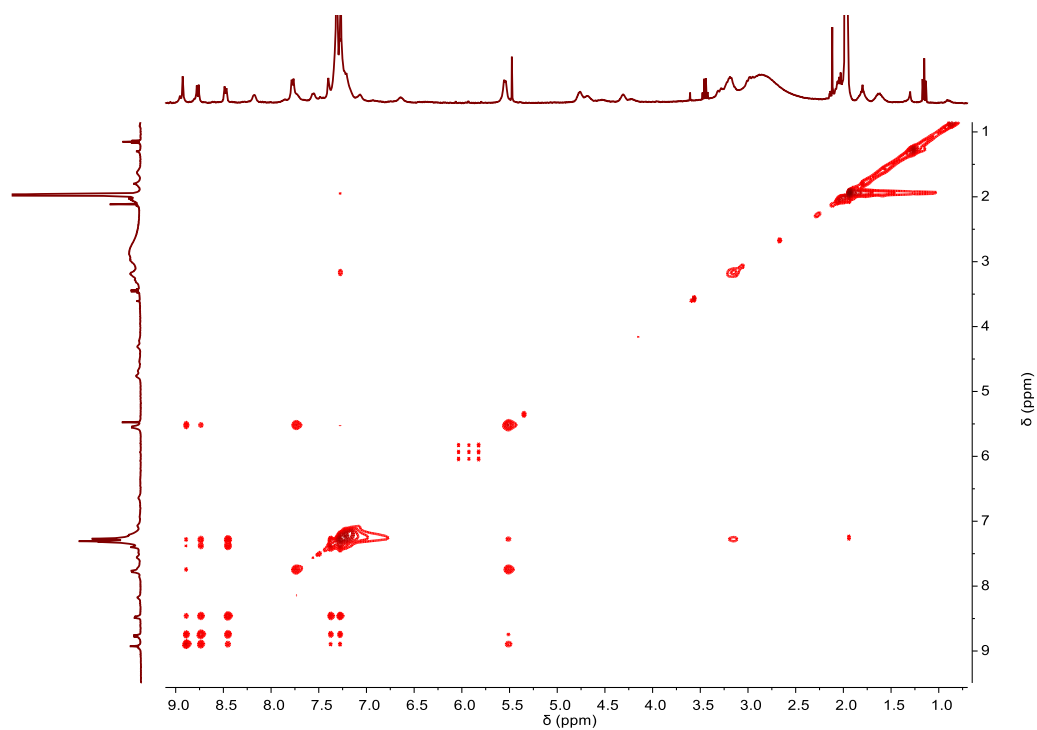


Figure S38: NOESY spectrum (500 MHz, 298 K, CD₃CN) of **3**.

SUPPORTING INFORMATION

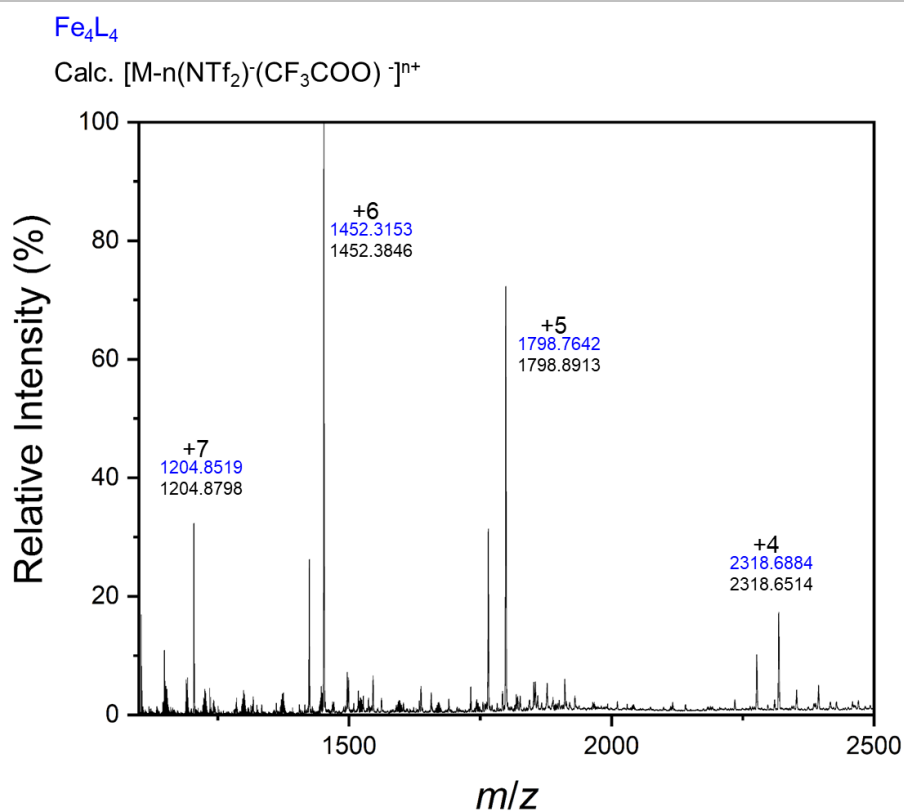


Figure S39: High-resolution ESI-MS spectrum of **3** in CH_3CN . Experimental (blue) and calculated (black) peaks.

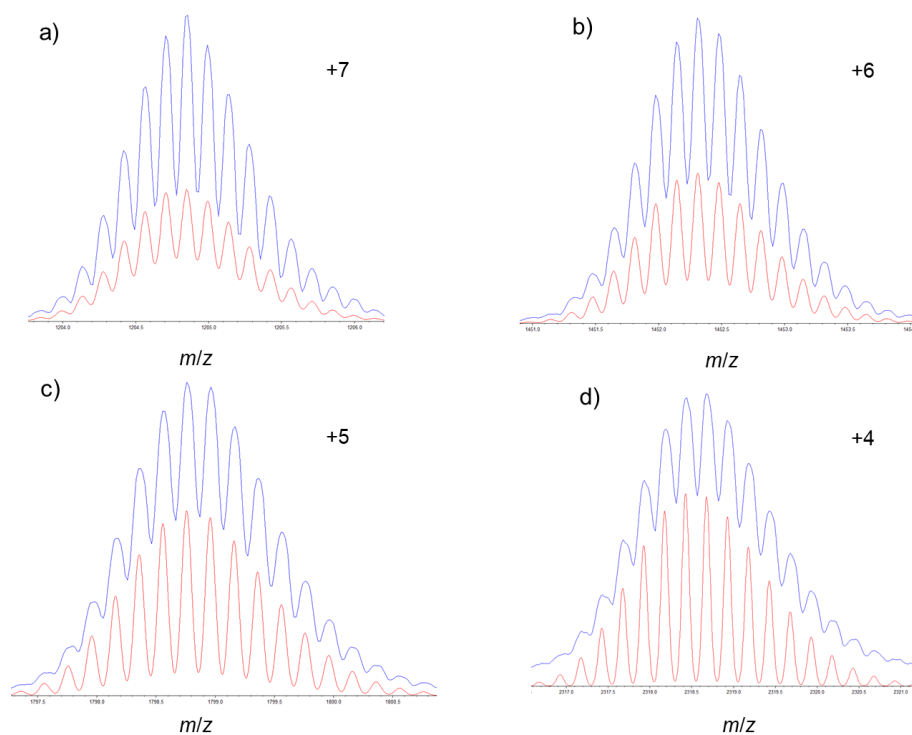


Figure S40: High-resolution ESI-MS spectra of **3** in CH_3CN . Experimental (blue) and calculated (red) peaks for a) $[\text{3}(\text{CF}_3\text{COO})]^{7+}$ b) $[\text{3}(\text{NTf}_2)(\text{CF}_3\text{COO})]^{6+}$ c) $[\text{3}(\text{NTf}_2)_2(\text{CF}_3\text{COO})]^{5+}$ d) $[\text{3}(\text{NTf}_2)_3(\text{CF}_3\text{COO})]^{4+}$.

SUPPORTING INFORMATION

2.9) Circular Dichroism

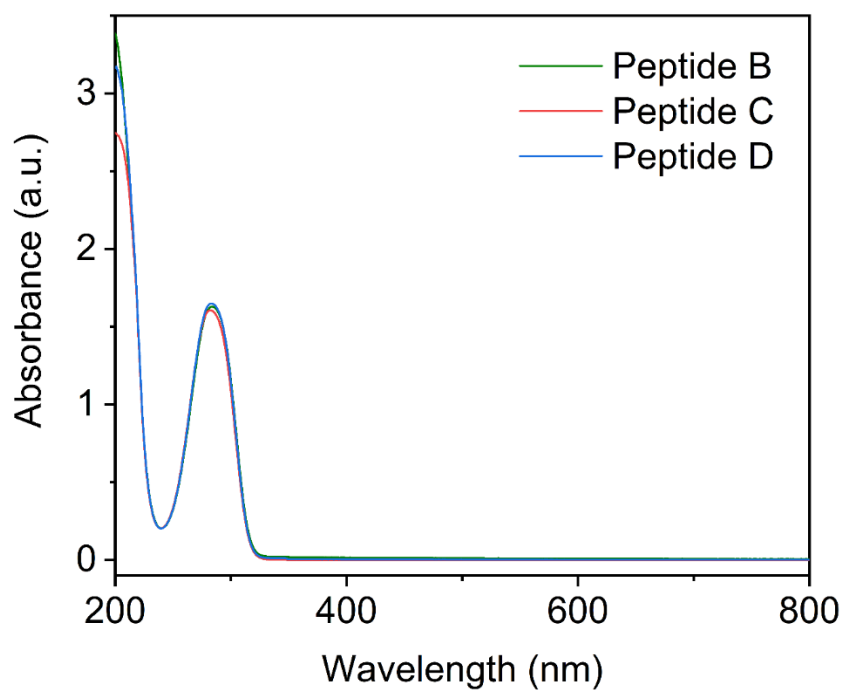


Figure S41: UV spectra of peptide B, C and D ([peptide]= 1.09 mM, CH₃CN, 298 K).

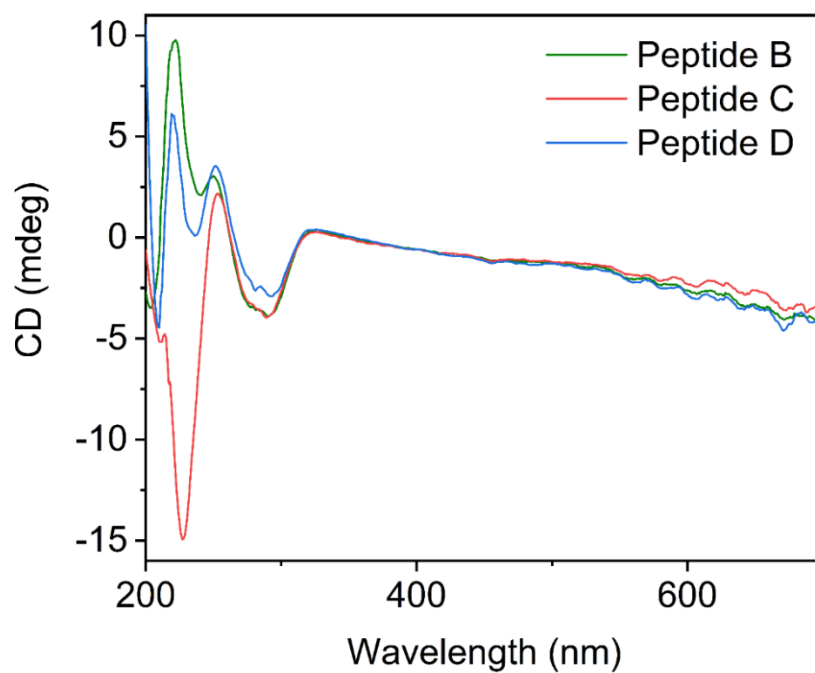


Figure S42: CD spectra of peptide B, C and D ([peptide]= 1.09 mM, CH₃CN, 298 K).

SUPPORTING INFORMATION

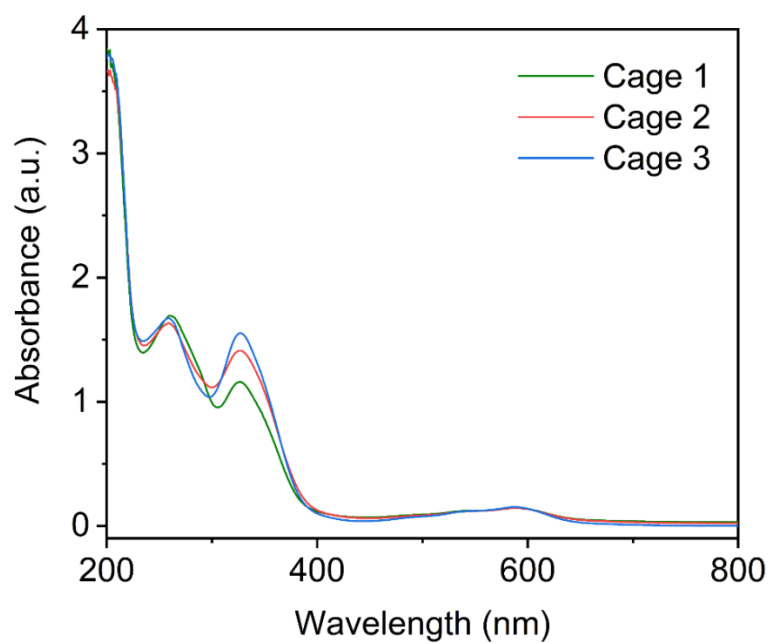


Figure S43: UV-visible spectrum for cage 1, 2 and 3 ([cage]= 0.08 mM, CH₃CN, 298 K).

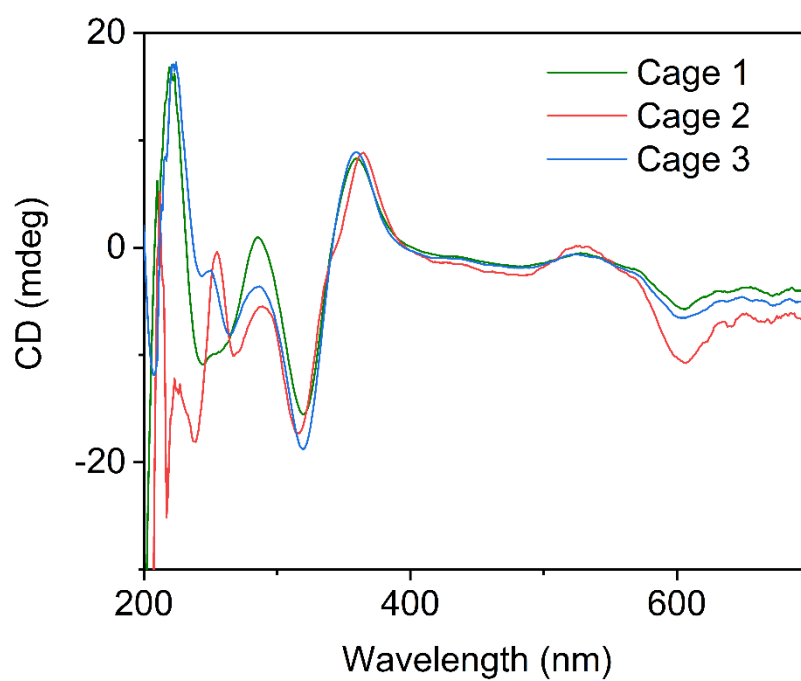


Figure S44: CD spectra of cage 1, 2 and 3 ([cage]= 0.08 mM, CH₃CN, 298 K).

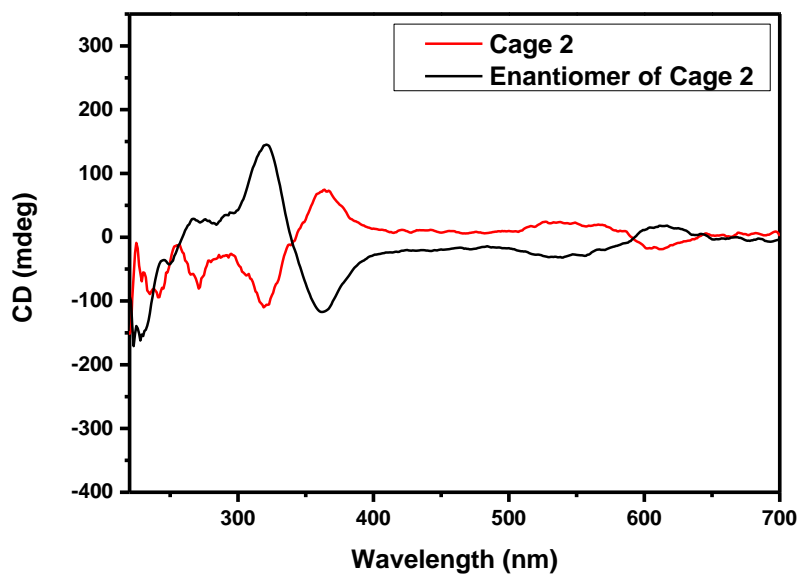


Figure S45: CD spectra of cage 2 and the correspondent enantiomer ([cage]= 0.08 mM, CH₃CN, 298 K).

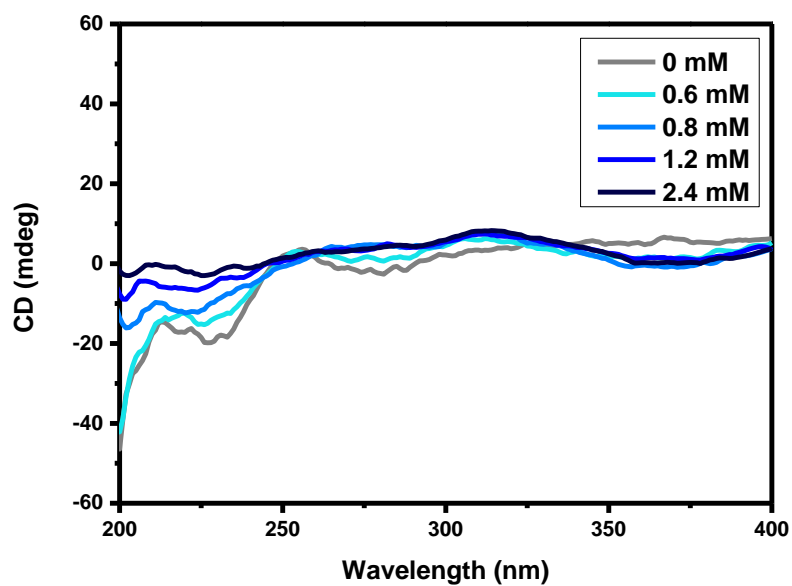


Figure S46: CD spectra of peptide C analog, *N*-Ac-L-Phe-D-Phe-L-Cys-NH₂ (1.2 mM) and different Ag⁺ concentrations (0.6, 0.8, 1.2, 2.4 mM).

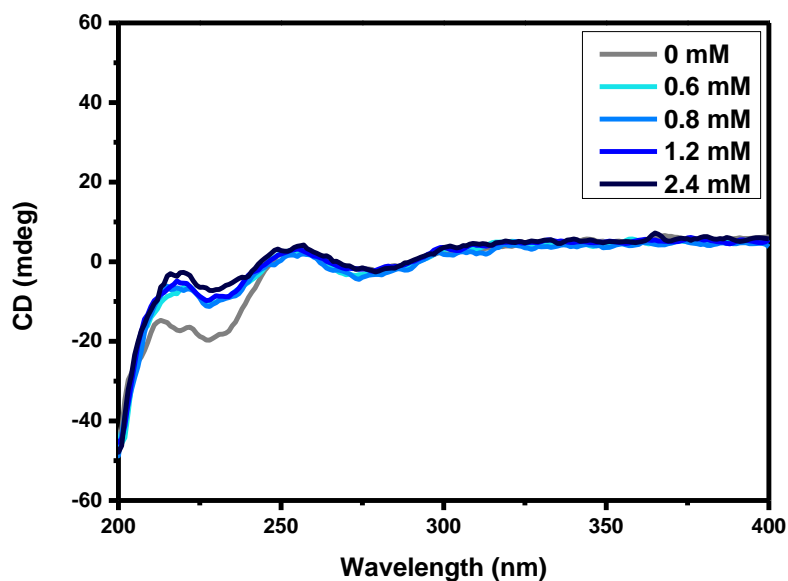


Figure S47: CD spectra of peptide C analog, *N*-Ac-L-Phe-D-Phe-L-Cys-NH₂ (1.2 mM) and different Zn²⁺ concentrations (0.6, 0.8, 1.2, 2.4 mM).

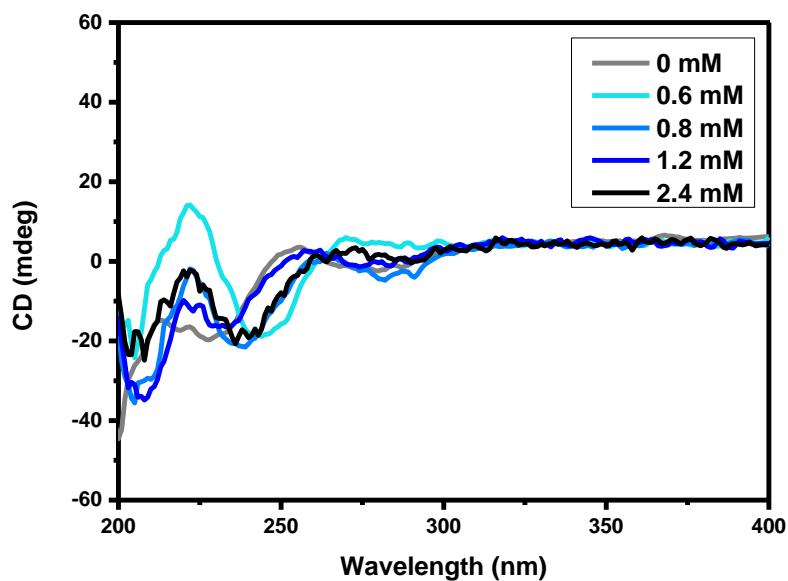


Figure S48: CD spectra of peptide C analog, *N*-Ac-L-Phe-D-Phe-L-Cys-NH₂ (1.2 mM) and different Hg²⁺ concentrations (0.6, 0.8, 1.2, 2.4 mM).

SUPPORTING INFORMATION

3) Gels formation and characterization

3.1) General preparation of cage gel

15 mg of Cage 1, 2 and 3 were dissolved in acetonitrile and sonicating in an ultrasonic bath by heating, respectively. The samples were left to cool down to room temperature and the gels were not formed.

Table S1. Attempts for the preparation of the cage gel.

	Concentration (mM)	Gel	Time for gelation
Cage 1	1.27 mM	NO	Solution even after 24 h
	2.5 mM	NO	Solution even after 24 h
	5 mM	NO	Solution even after 24 h
Cage 2	1.27 mM	NO	Solution even after 24 h
	2.5 mM	NO	Solution even after 24 h
	5 mM	NO	Solution even after 24 h
Cage 3	1.27 mM	NO	Solution even after 24 h
	2.5 mM	NO	Solution even after 24 h
	5 mM	NO	Solution even after 24 h

3.2) General preparation of cage gels triggered by metal ions

Stock solutions of 5 mM cages 1 and 2 were prepared in acetonitrile. Then, different metal salts were added to the required volume of the cage solution to obtain the desired final concentrations of metal ions of 30, 60, 90 mM, respectively and cage of 5 mM. The sample was ultrasonicated for two minutes.

Table S2. Attempts for the preparation of cage gel triggered by different metal ions at different concentrations.

Cage	Metals	Concentration (mM)	Gelation	Observations	
1		30 mM	NO		
		60 mM	NO		
		90 mM	NO		
	Zn ²⁺	30 mM	NO		
		60 mM	NO		
		90 mM	NO		
2	Hg ²⁺	30 mM	NO		
		60 mM	NO		
		90 mM	YES	Leave for 2 days	
	Ag ⁺	30 mM	30 mM	YES	Minimum Gelation Concentration
			60 mM	YES	Sonication 30 seconds ^[a]
			90 mM	YES	Sonication 30 seconds ^[a]
60 mM		30 mM	YES	Sonication 30 seconds ^[a]	
		60 mM	YES	Sonication 30 seconds ^[a]	
		90 mM	YES	Sonication 30 seconds ^[a]	
90 mM		30 mM	YES	Sonication 30 seconds ^[a]	
		60 mM	YES	Sonication 30 seconds ^[a]	
		90 mM	YES	Sonication 30 seconds ^[a]	

^[a]The cage was dissolved in acetonitrile by heating. Then the metal ions were added to get a final concentration of 5 mM cage with different concentrations of metal ions and it was sonicated for the indicated time to get the gel.

SUPPORTING INFORMATION

3.3) Oscillatory rheometry of Cage 2 gel triggered by metal ions

Table S3. Elastic (G') and viscous (G'') moduli for the different gels described here. The values shown in the table are calculated as the average (standard deviation included) of 3 independent experiments performed using 3 different samples. The cage concentration was kept at 5 mM and metal ions at 30 mM for the different hybrid gels.

	G' (Pa)	G'' (Pa)	Shear modulus (Pa)	Broken stress (Pa)	γ_c (%)
Ag	1297±34	255±83	1626	22	2.78
Zn	2225±312	683±67	3209	68	1.67
Hg	3507±708	591±39	3867	68	1.03

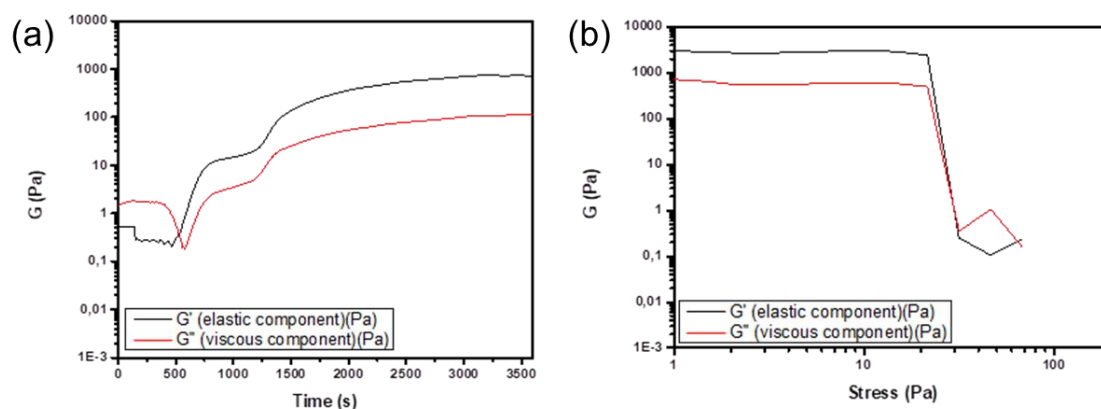


Figure S49: Oscillatory rheometry analysis of Ag^+ regulated gel timesweep (a) and stress sweep (b), with the elastic modulus (G') in black and the viscous modulus (G'') in red.

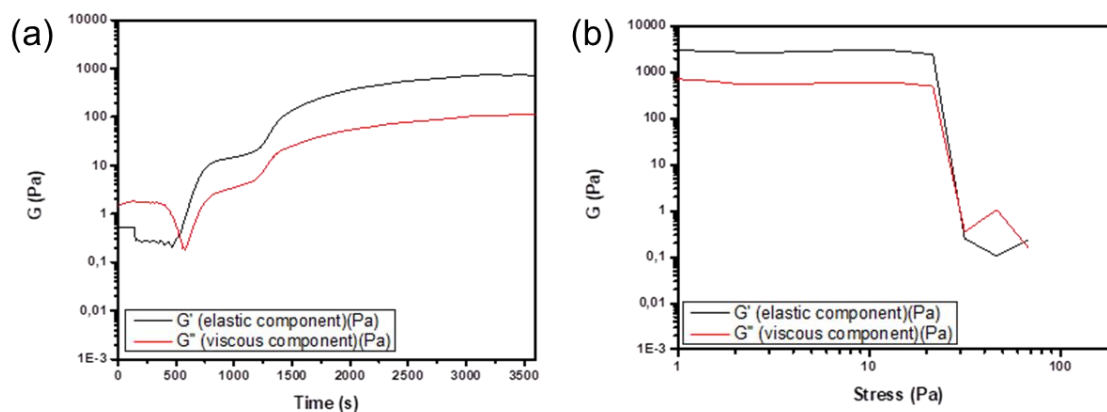


Figure S50: Oscillatory rheometry analysis of Zn^{2+} regulated gel time sweep (a) and stress sweep (b), with the elastic modulus (G') in black and the viscous modulus (G'') in red.

SUPPORTING INFORMATION

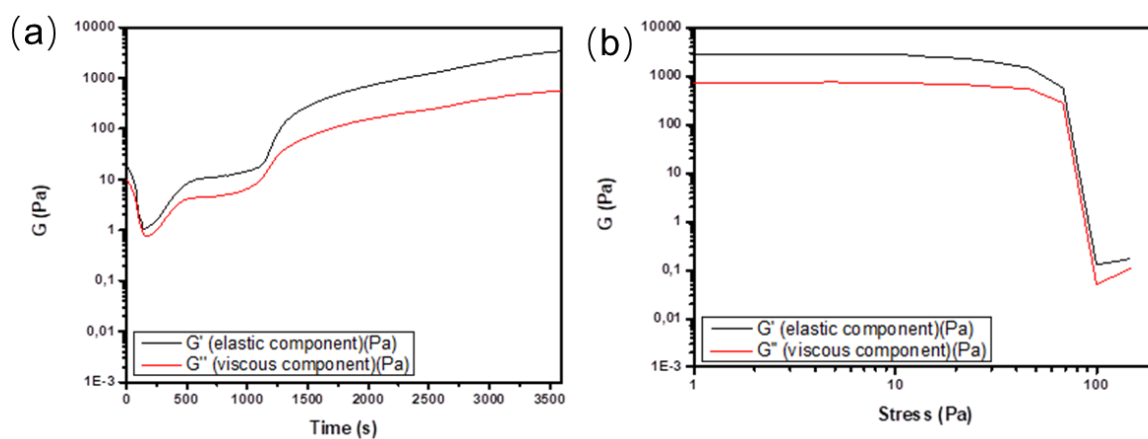


Figure S51: Oscillatory rheometry analysis of Hg^{2+} regulated gel time sweep (a) and stress sweep (b), with the elastic modulus (G') in black and the viscous modulus (G'') in red.

3.4) TEM characterization

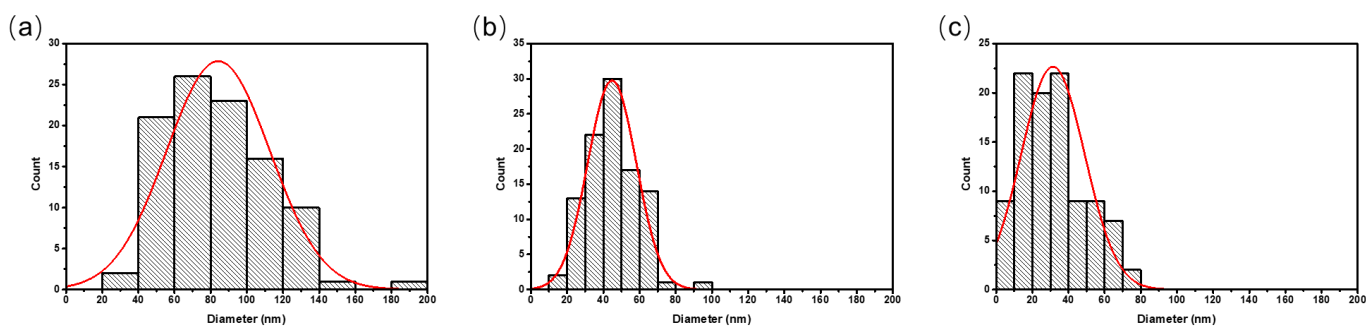


Figure S52: Nanomorphological size distribution analyses of TEM micrographs of gels prepared by 2 and different metal additives: (a) Ag^+ , (b) Zn^{2+} , and (c) Hg^{2+} .

SUPPORTING INFORMATION

3.5) Raman spectroscopy

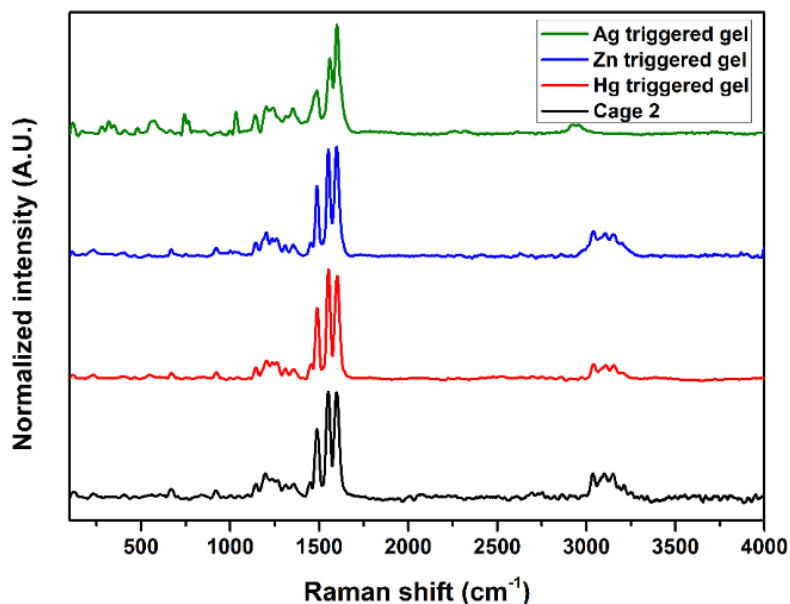


Figure S53: Raman characterization including Raman spectra of Cage 2 and the gels triggered by different metal ions.

The medium intensity bands with four peaks in the region 3030-3200 cm^{-1} are relative to overlapping of aromatic C-H stretching vibrations and much broader N-H stretching vibrations. Intense bands between 1493 and 1600 cm^{-1} , which were attributed to C=N and N-Fe stretching. The weak signals in the region are due to aromatic =C-H in-plane deformation vibrations.

3.6) XPS analysis

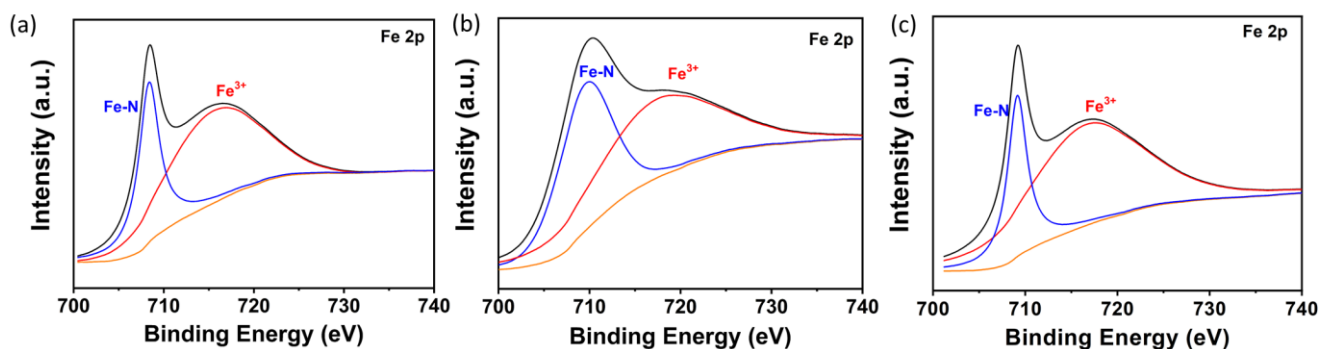


Figure S54: XPS characterizations of three gels with Fe 2p XPS spectra of Ag⁺ regulated gel (a); Zn²⁺ regulated gel (b); Hg²⁺ regulated gel (c).

SUPPORTING INFORMATION

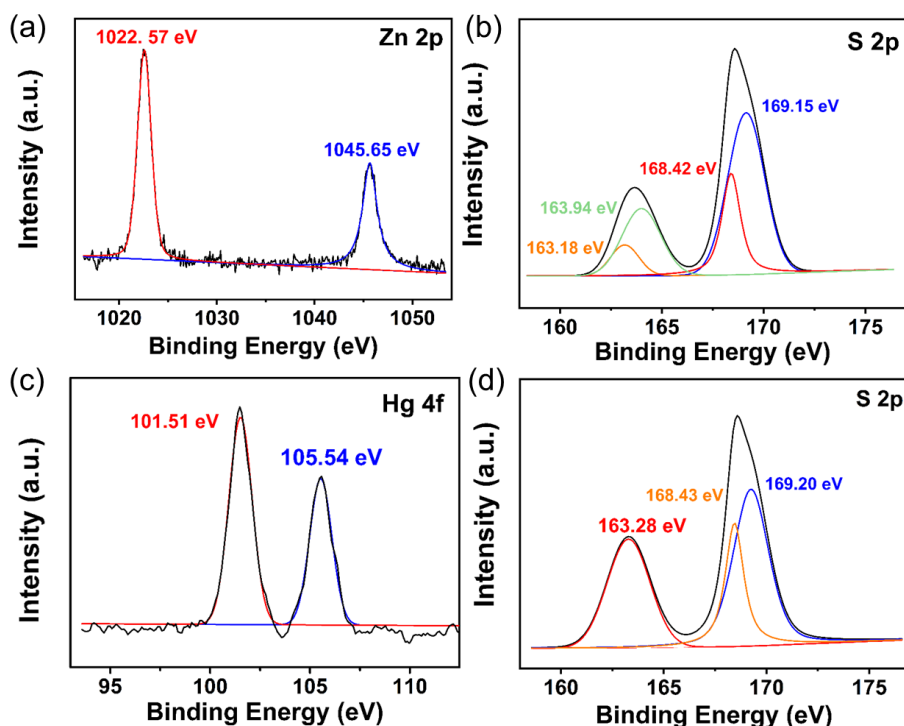


Figure S55: XPS analysis of three cage-peptide gels prepared from **2**. (a) and (c) are XPS spectra corresponding to Zn 2p, and Hg 4f, respectively, and (b) and (d) are the S 2p XPS spectra for the same samples shown in (a) and (c), confirming the presence of Tf₂N⁻ in each case.

In the Zn²⁺-triggered gel, binding energy values for Zn 2p_{3/2} and Zn 2p_{1/2} were found at 1022.62 eV and 1045.65 eV. Peaks at 163.18 and 163.94 eV are assigned to the zinc-bound sulfur in Cys (Figure S54a).^[S3] The peaks at 168.42 and 169.15 eV of S 2p_{1/2} were attributed to sulfur atoms in Tf₂N⁻ (Figure S54b). Hg 4f₅ and Hg 4f₇ spectra of the metallo gel containing Hg²⁺ displayed the peaks at 101.51 and 105.54 eV that were attributed to Cys-bound mercury (Figure S54c). The characteristic peak at 163.28 eV provided further evidence for interactions between S and Hg²⁺.^[S4] The signals at 168.43 and 169.20 eV of S 2p_{1/2} were attributed to sulfur atoms in NTf₂⁻ (Figure S54d).

References:

- [S1] M. Kieffer, A. M. Garcia, C. J. Haynes, S. Kralj, D. Iglesias, J. R. Nitschke, S. Marchesan, *Angew. Chem. Int. Ed.* **2019**, *58*, 7982-7986; *Angew. Chem.* **2019**, *131*, 8066-8070.
- [S2] J. Zhu, Z. Yan, F. Bošković, C. Haynes, M. Kieffer, J. Greenfield, J. Wang, J. R. Nitschke, U. F. Keyser, *Chem. Sci.*, **2021**, *12*, 14564-14569.
- [S3] M. Madkour, Y. Abdelmonem, U. Y. Qazi, R. Javaid, S. Vadivel, *RSC Adv.* **2021**, *11*, 29433-29440.
- [S4] F. Jia, C. Liu, B. Yang, X. Zhang, H. Yi, J. Ni, S. Song, *ACS Sustain. Chem. Eng.* **2018**, *6*, 9065-9073.

CRedit:

Data investigation (ML, HZ, SA, WX, AH, AMG, SK), Conceptualization (JRN and SM), Writing- Initial draft (ML), Writing- Review and Editing (ML, HZ, SA, WX, AH, AMG, SK, JRN and SM).